Supporting Information

# Amino-functionalized MOFs with high physicochemical stability for efficient gas storage/separation, dye adsorption and catalytic performance

Weidong Fan,[a] Xia Wang,[a] Ben Xu,[a] Yutong Wang,[a] Dandan Liu,[b] Ming Zhang,[a] Yizhu Shang,[a] Fangna Dai,[a] Liangliang Zhang[a] and Daofeng Sun*[a]

[a] School of Materials Science and Engineering, College of Science, China University of Petroleum (East China), Qingdao, Shandong 266580, People's Republic of China

[b] Research Centre of New Energy Science and Technology, Research Institute of Unconventional Oil & Gas and Renewable Energy, China University of Petroleum (East China), Qingdao, Shandong 266580, People's Republic of China

Email: dfsun@upc.edu.cn

**DOI: 10.1039/x0xx00000x**

# Table of Contents

**1. Synthesis of $H_4$DCBA**

**2. Crystal data, structure and characterization of UPC-100-In, UPC-101-Al, and UPC-102-Zr.**

**3. Gas adsorption of UPC-100-In, UPC-101-Al, and UPC-102-Zr.**

**4. Dye adsorption of UPC-102-Zr.**

**5. Catalyze Knoevenagel condensation reactions of UPC-100-In, UPC-101-Al, and UPC-102-Zr.**

## 1. Synthesis of $H_4$DCBA

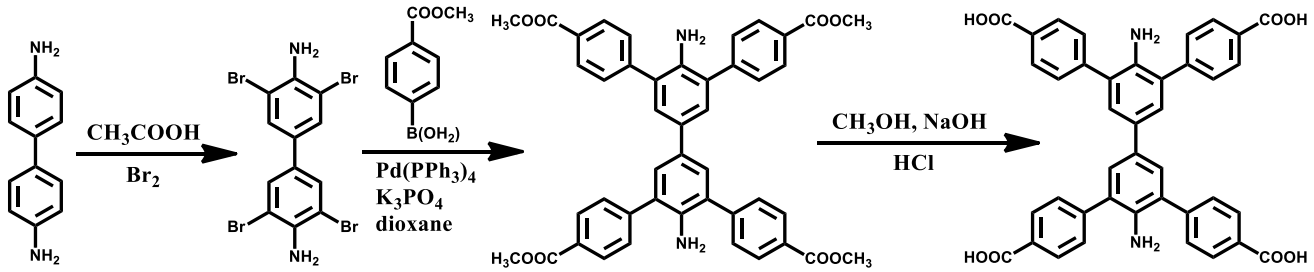


**Scheme S1.** Synthetic procedures of the $H_4$DCBA ligand.

**3,3',5,5'-tetrabromo-[1,1'-biphenyl]-4,4'-diamine**

A sample of benzidine (1.0 g, 2.0 mmol) was dissolved in 30 ml of glacial acetic acid at room temperature. Bromine (1.2 ml) was added slowly with rapid stirring and then the mixture was continue stirred for 4 h. The brown precipitate was filtered off, washed with water several times, and dried in vacuum (yield: 83%). $^1$H NMR (400 MHz, $CDCl_3$) 5.31 (s, 4H), 7.53 (s, 4H). Anal. Calcd. for $C_{12}H_8Br_4N_2$ (mw 496): C, 28.84; H, 1.16; N, 5.60. Found: C, 28.80; H, 1.12; N, 5.63.

**Dimethyl 4'',6'-diamino-5',5''-bis(4-(methoxycarbonyl)phenyl)-[1,1':3',1'':3'',1'''-quarterphenyl]-4,4'''-dicarboxylate**

3,3',5,5'-tetrabromo-[1,1'-biphenyl]-4,4'-diamine (1.98 g, 4 mmol), Methyl 4-boronobenzoate (3.14 g, 19.2 mmol), $Pd(PPh_3)_4$ (0.30 g, 0.26 mmol) and $K_3PO_4$ (3.82 g, 18.0 mmol) were placed in a 500 ml two-necked round bottom flask under a $N_2$ gas atmosphere. The flask was further charged with a 200 mL of dry 1,4-dioxane, and the contents were heated for 48 h. After the mixture was cooled to room temperature, the solvent was removed, water was added. The water phase was washed with $CH_2Cl_2$. The mixed organic phases were dried with $MgSO_4$. After the solvent was removed, the crude product was purified by column chromatography with $CH_2Cl_2$ as the eluent. $^1$H NMR (400 MHz, $CDCl_3$) 3.95(s, 12H), 5.31(s, 4H), 7.37(d, 8H), 8.13(d, 8H). Anal. Calcd. for $C_{44}H_{36}N_2O_8$ (mw 720): C, 73.32; H, 5.03; N, 3.89. Found: C, 73.37; H, 5.01; N, 3.93.

**4'',6'-diamino-5',5''-bis(4-carboxyphenyl)-[1,1':3',1'':3'',1'''-quaterphenyl]-4,4'''-dicarboxylic acid**

Dimethyl 4",6'-diamino-5',5"-bis(4-(methoxycarbonyl)phenyl)-[1,1':3',1":3",1'"-quarterphenyl]-4,4'"-dicarboxylate (2.0 g, 2.8 mmol) was dissolved in 50 ml MeOH, 50 ml 2 M NaOH aqueous solution was added. The mixture was stirred at 50 ℃ overnight. The organic phase was removed, the aqueous phase was acidified with diluted hydrochloric acid to give yellow precipitate, which was filtered and wased with

water several times. $^1$H NMR (400 MHz, $CDCl_3$) 4.46(s, 4H), 7.46(s, 4H), 7.69(d, 8H), 8.03(d, 8H). Anal. Calcd. for $C_{40}H_{28}N_2O_8$ (mw 664): C, 72.28; H, 4.25; N, 4.21. Found: C, 72.30; H, 4.30; N, 4.15.

**2. Crystal data, structure and characterization of UPC-100-In, UPC-101-Al, and UPC-102-Zr.**

**Table S1.** Crystal data and structure refinement of **UPC-100-In**, **UPC-101-Al**, and **UPC-102-Zr**.

| Identification code | **UPC-100-In** | **UPC-101-Al** | **UPC-102-Zr** |
|---|---|---|---|
| Empirical formula | $C_{40}H_{24}N_2O_8In$ | $C_{40}H_{26}N_2O_{10}Al_2$ | $C_{80}H_{64}N_4O_{32}Zr_6$ |
| Formula weight | 775.45 | 748.59 | 2140.67 |
| Temperature/K | 150(10) | 293(2) | 293(2) |
| Crystal system | monoclinic | orthorhombic | hexagonal |
| Space group | C2/c | Cmmm | P6/mmm |
| a/Å | 12.7988(18) | 6.5926(3) | 40.9189(8) |
| b/Å | 30.8674(10) | 29.493(2) | 40.9189(8) |
| c/Å | 15.6757(9) | 15.9919(9) | 15.1257(5) |
| α/° | 90 | 90 | 90 |
| β/° | 112.407(11) | 90 | 90 |
| γ/° | 90 | 90 | 120 |
| Volume/Å$^3$ | 5725.4(10) | 3109.4(3) | 21932.8(9) |
| Z | 4 | 2 | 3 |
| $\rho_{calc}$ mg/mm$^3$ | 0.902 | 0.800 | 0.486 |
| μ/mm$^{-1}$ | 3.590 | 0.736 | 1.907 |
| F(000) | 1572 | 772 | 3204.0 |
| 2Θ range for data | 4.001 to 70.781° | 8.16 to 131.86° | 7.26 to 132.1° |
| Reflections collected | 10661 | 4007 | 52032 |
| Independent reflections | 5344 [Rint = 0.0234, Rsigma = 0.0788] | 1554 [Rint = 0.0439, Rsigma = 0.0727] | 7128 [Rint = 0.2059, Rsigma = 0.1659] |
| Data/restraints/parameters | 5344/364/220 | 1554/0/104 | 7128/1/152 |
| Goodness-of-fit on F$^2$ | 1.341 | 1.402 | 1.060 |
| Final R indexes [I>=2σ (I)] | R1 = 0.1310, wR2 = 0.3566 | R1 = 0.1431, wR2 = 0.3756 | R1 = 0.0726, wR2 = 0.1358 |
| Final R indexes [all data] | R1 = 0.1572, wR2 = 0.3822 | R1 = 0.1841, wR2 = 0.4190 | R1 = 0.1187, wR2 = 0.1446 |
| Largest diff. peak/hole /e | 1.288/-0.875 | 0.97/-0.75 | 1.14/-1.05 |

**Table S2.** Selected bond lengths (Å) and selected bond angles (º) for **UPC-100-In**.

| Atom | Atom | Length/Å | Atom | Atom | Atom | Angle/° |
|---|---|---|---|---|---|---|
| In1 | O1 | 2.282(9) | O1[1] | In1 | O1 | 109.1(4) |
| In1 | O1[1] | 2.282(9) | O1[1] | In1 | O4[2] | 139.2(4) |
| In1 | O4[2] | 2.284(7) | O1 | In1 | O4[2] | 91.8(3) |
| In1 | O4[3] | 2.284(7) | O1 | In1 | O4[3] | 139.2(4) |
| In1 | O2[1] | 2.252(9) | O1[1] | In1 | O4[3] | 91.8(3) |
| In1 | O2 | 2.252(9) | O4[3] | In1 | O4[2] | 94.4(5) |
| In1 | O3[2] | 2.232(8) | O2 | In1 | O1 | 54.8(4) |
| In1 | O3[3] | 2.232(8) | O2[1] | In1 | O1 | 80.7(3) |
| | | | O2[1] | In1 | O1[1] | 54.8(4) |
| | | | O2 | In1 | O1[1] | 80.7(3) |
| | | | O2 | In1 | O4[3] | 166.0(4) |
| | | | O2[1] | In1 | O4[2] | 166.0(4) |

Symmetry transformations used to generate equivalent atoms:

[1]-x+1,y,-z+1/2; [2]x+1/2,y-1/2,z; [3]-x+1/2,y-1/2,-z+1/2; [4]-x+1,y,-z+3/2; [5]x-1/2,y+1/2,z

**Table S3.** Selected bond lengths (Å) and selected bond angles (º) for **UPC-101-Al**.

| Atom | Atom | Length/Å | Atom | Atom | Atom | Angle/° |
|---|---|---|---|---|---|---|
| Al1 | O1[1] | 1.889(3) | O1[1] | Al1 | O1[2] | 92.14(19) |
| Al1 | O1[2] | 1.889(3) | O1[2] | Al1 | O1[3] | 87.86(19) |
| Al1 | O1 | 1.889(3) | O1[1] | Al1 | O1[3] | 180.00(15) |
| Al1 | O1[3] | 1.889(3) | O1[1] | Al1 | O1 | 87.86(19) |
| Al1 | O2[3] | 1.822(2) | O1[2] | Al1 | O1 | 180.00(19) |
| Al1 | O2 | 1.822(2) | O1 | Al1 | O1[3] | 92.14(19) |
| | | | O2 | Al1 | O1 | 91.71(16) |
| | | | O2 | Al1 | O1[3] | 91.71(16) |
| | | | O2[2] | Al1 | O1[2] | 91.71(16) |
| | | | O2[2] | Al1 | O1 | 88.29(16) |
| | | | O2 | Al1 | O1[2] | 88.29(16) |
| | | | O2 | Al1 | O1[1] | 88.29(16) |
| | | | O2[2] | Al1 | O1[1] | 91.71(16) |
| | | | O2[2] | Al1 | O1[3] | 88.29(16) |
| | | | O2 | Al1 | O2[2] | 180.0(3) |

Symmetry transformations used to generate equivalent atoms:

[1]1/2-X,1/2-Y,+Z; [2]1/2-X,1/2-Y,-Z; [3]+X,+Y,-Z; [4]1/2+X,1/2-Y,-Z; [5]1-X,+Y,+Z; [6]+X,+Y,1-Z; [7]1-X,-Y,1-Z

**Table S4.** Selected bond lengths (Å) and selected bond angles (º) for **UPC-102-Zr**.

| Atom | Atom | Length/Å | Atom | Atom | Atom | Angle/° |
|---|---|---|---|---|---|---|
| Zr1 | Zr2$^{1}$ | 3.4995(8) | Zr2$^{1}$ | Zr1 | Zr2 | 60.89(2) |
| Zr1 | Zr2 | 3.4995(8) | Zr2 | Zr1 | Zr2$^{2}$ | 60.46(3) |
| Zr1 | Zr2$^{2}$ | 3.4995(8) | Zr2$^{3}$ | Zr1 | Zr2$^{2}$ | 60.89(2) |
| Zr1 | Zr2$^{3}$ | 3.4995(8) | Zr2$^{3}$ | Zr1 | Zr2 | 91.17(3) |
| Zr1 | O1$^{4}$ | 2.125(3) | Zr2$^{1}$ | Zr1 | Zr2$^{2}$ | 91.17(3) |
| Zr1 | O1 | 2.125(3) | Zr2$^{1}$ | Zr1 | Zr2$^{3}$ | 60.46(3) |
| Zr1 | O15 | 2.125(3) | O1$^{2}$ | Zr1 | Zr2$^{1}$ | 166.47(11) |
| Zr1 | O1$^{3}$ | 2.125(3) | O1 | Zr1 | Zr2 | 75.30(10) |
| Zr1 | O3 | 2.140(4) | O1 | Zr1 | Zr2$^{2}$ | 110.95(10) |
| Zr1 | O3$^{3}$ | 2.140(4) | O1 | Zr1 | Zr2$^{1}$ | 111.16(10) |
| Zr1 | O4 | 2.101(4) | O1$^{4}$ | Zr1 | Zr2 | 166.47(11) |
| Zr1 | O4$^{4}$ | 2.101(4) | O1$^{5}$ | Zr1 | Zr2$^{1}$ | 75.30(10) |
| Zr2 | Zr1$^{2}$ | 3.4995(8) | O1$^{4}$ | Zr1 | Zr2$^{2}$ | 111.16(10) |
| Zr2 | Zr2$^{3}$ | 3.5235(15) | O1$^{4}$ | Zr1 | Zr2$^{1}$ | 110.95(10) |
| Zr2 | Zr2$^{1}$ | 3.5463(13) | O1$^{5}$ | Zr1 | Zr2 | 111.16(10) |
| Zr2 | O2$^{6}$ | 2.201(4) | O1$^{2}$ | Zr1 | Zr2$^{3}$ | 111.16(10) |
| Zr2 | O2 | 2.201(4) | O1$^{2}$ | Zr1 | Zr2$^{2}$ | 75.30(10) |
| Zr2 | O3$^{1}$ | 2.084(2) | O1 | Zr1 | Zr2$^{3}$ | 166.47(11) |
| Zr2 | O3 | 2.084(2) | O1$^{5}$ | Zr1 | Zr2$^{2}$ | 166.47(11) |
| Zr2 | O4 | 2.107(2) | O1$^{5}$ | Zr1 | Zr2$^{3}$ | 110.95(10) |
| Zr2 | O4$^{7}$ | 2.107(2) | O1$^{4}$ | Zr1 | Zr2$^{3}$ | 75.30(10) |
| Zr2 | O5 | 2.255(4) | O1$^{2}$ | Zr1 | Zr2 | 110.95(10) |
| Zr2 | O6 | 2.128(5) | O1 | Zr1 | O1$^{4}$ | 118.2(2) |

Symmetry transformations used to generate equivalent atoms:

$^{1}$-Y+X,-Y,-Z; $^{2}$1-X,-Y,-Z; $^{3}$1+Y-X,+Y,+Z; $^{4}$+X,+Y,-Z; $^{5}$1+Y-X,+Y,-Z; $^{6}$-Y+X,-Y,+Z; $^{7}$1-X,-Y,+Z; $^{8}$+X,+X-Y,+Z; $^{9}$+X,+Y,1-Z

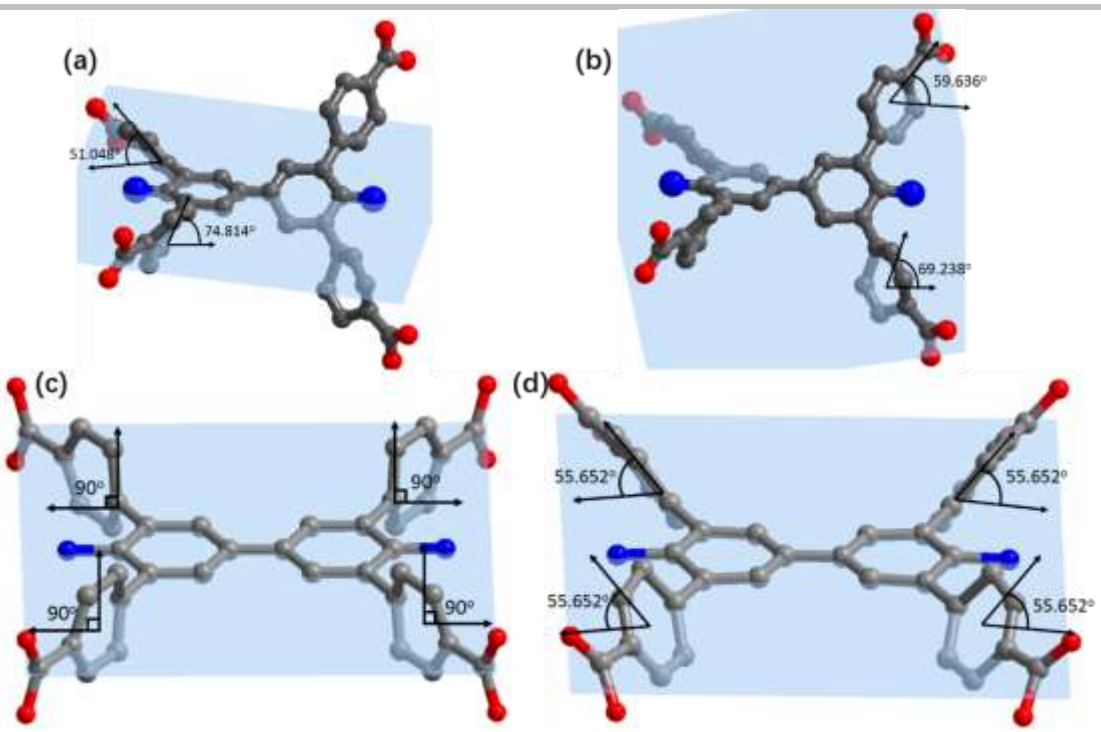


**Figure S1.** The dihedral angles between four sloping pendant benzene groups and the central benzene ring in DCBA for **UPC-100-In** (a and b), **UPC-101-Al** (c), and **UPC-102-Zr** (d).

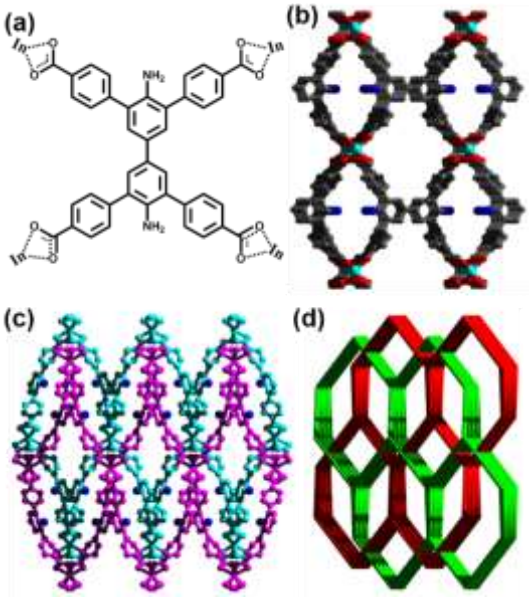


**Figure S2.** (a) Chemical structure. (b) Three-dimensional open framework along the a-axis. (c and d) two- fold interpenetrating framework and ***dia*** topology of **UPC-100-In.**

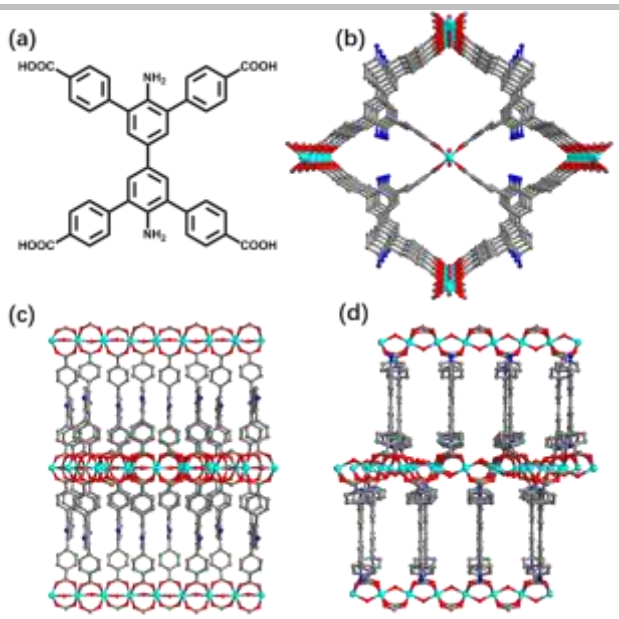


**Figure S3.** The structure of **UPC-101-Al:** (a) Chemical structure. (b) Three-dimensional open framework along the a-axis. (c) Three-dimensional open framework along the b-axis. (d) Three-dimensional open framework along the c-axis.

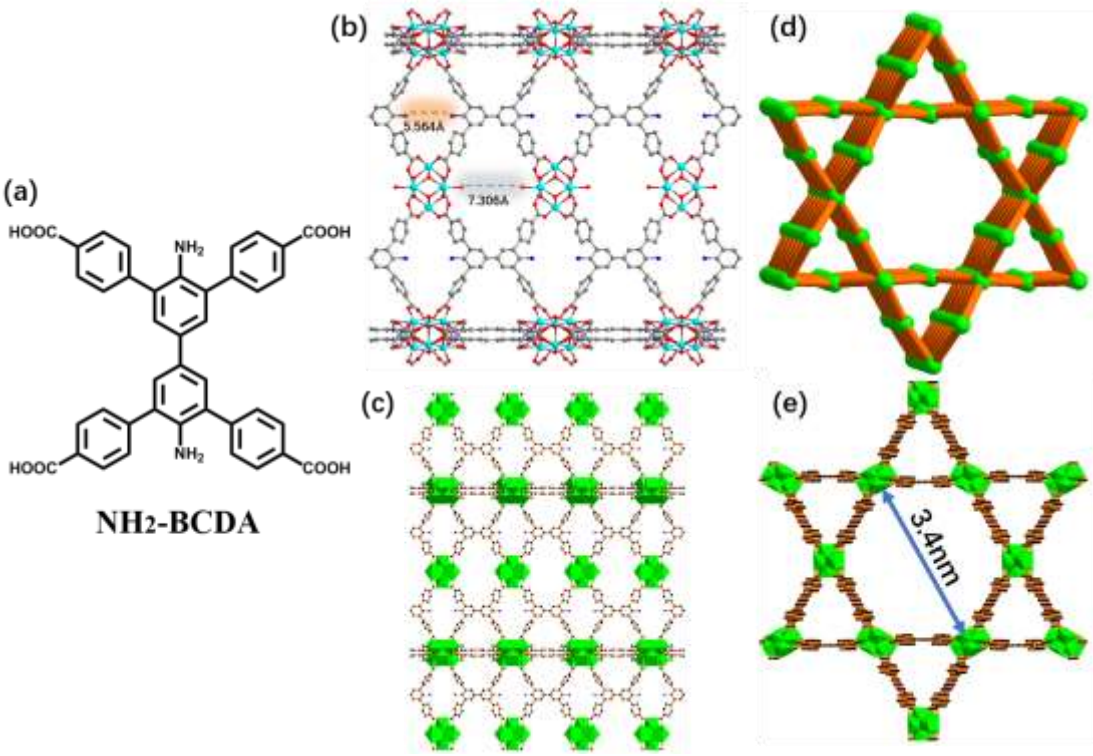


**Figure S4.** The structure of **UPC-102-Zr:** (a) Chemical structure. (b) and (c) Three-dimensional open framework along the a-axis. (d) and (e) Three-dimensional open framework along the c-axis.

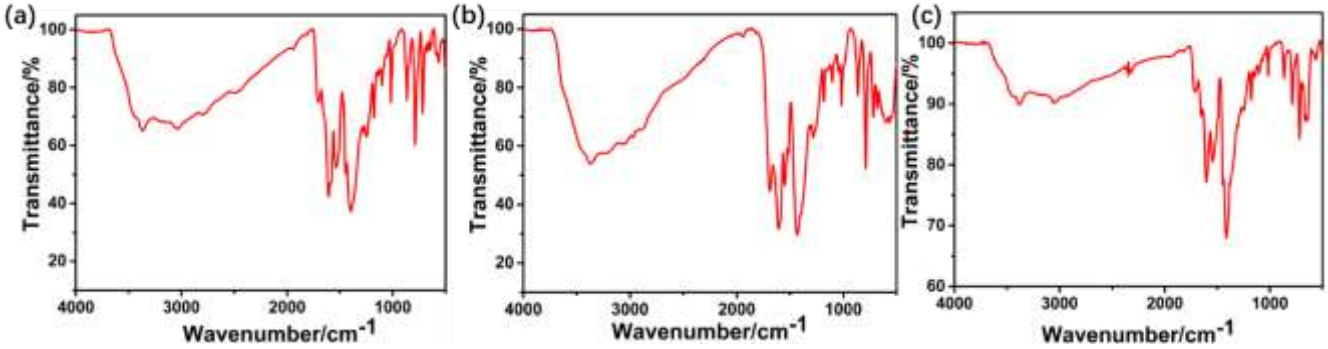


**Figure S5.** The IR of **UPC-100-In (a)**, **UPC-101-Al (b)**, and **UPC-102-Zr** (c).

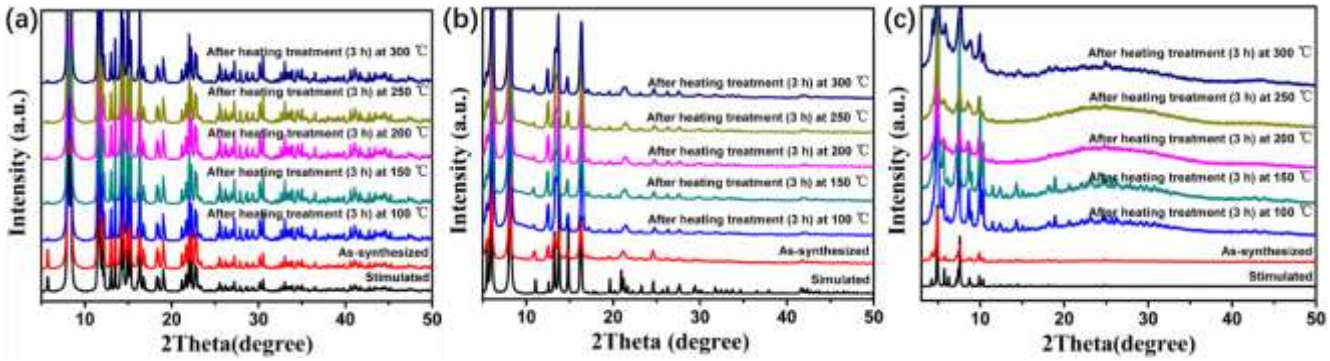


**Figure S6.** Powder X-ray diffraction (PXRD) of **UPC-100-In**, **UPC-101-Al**, and **UPC-102-Zr** under different temperatures.

## 3. Gas adsorption of UPC-100-In, UPC-101-Al, and UPC-102-Zr.

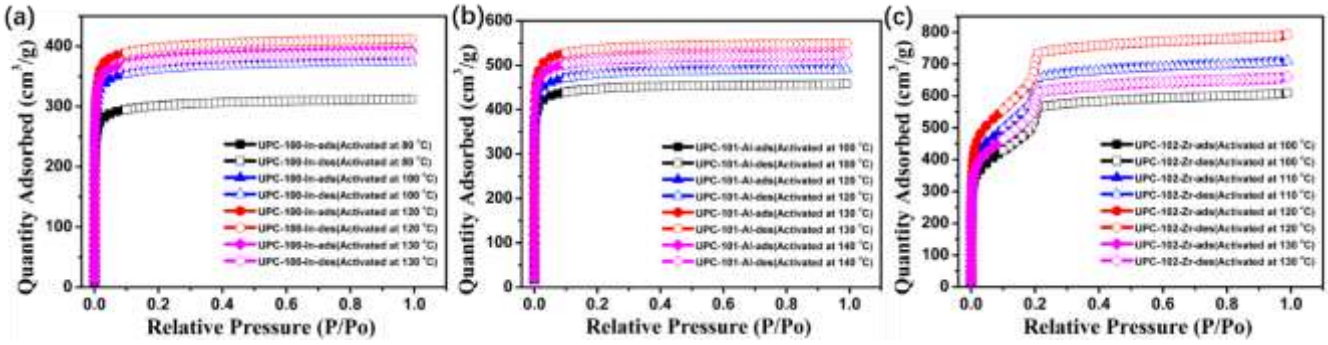


**Figure S7.** $N_2$ sorption isotherms of **UPC-100-In**, **UPC-101-Al**, and **UPC-102-Zr** under different activation temperatures.

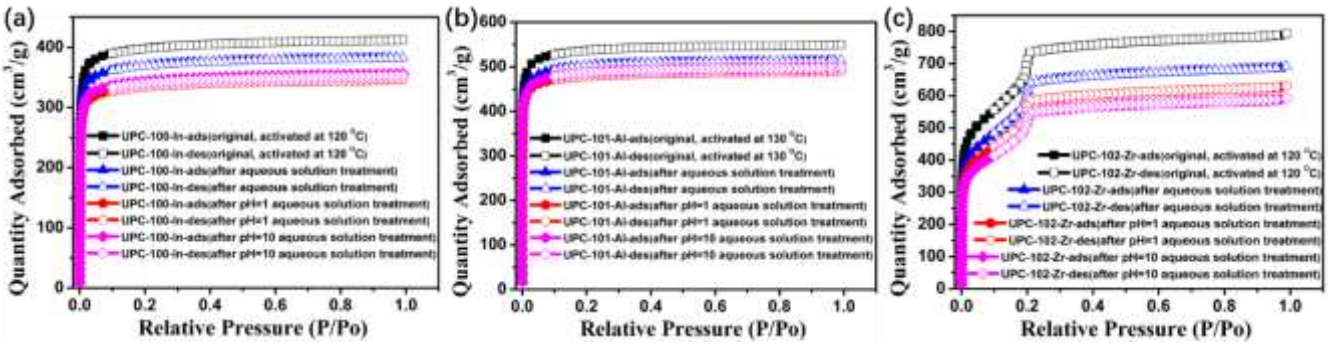


**Figure S8.** $N_2$ sorption isotherms of **UPC-100-In**, **UPC-101-Al**, and **UPC-102-Zr** under the treatment of water, acid (pH=1) and base (pH=10).

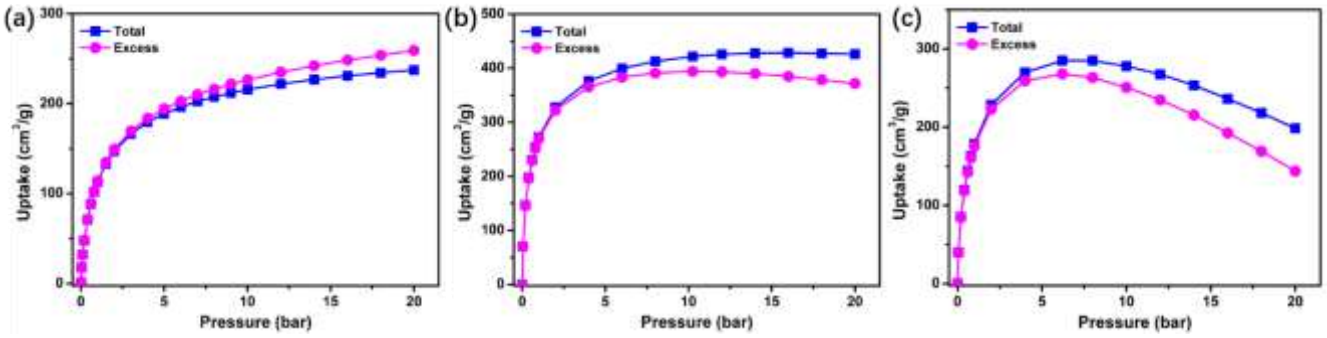


**Figure S9.** High-pressure $H_2$ total and excess uptake for **UPC-100-In**, **UPC-101-Al**, and **UPC-102-Zr** at 77 K and 20 bar.

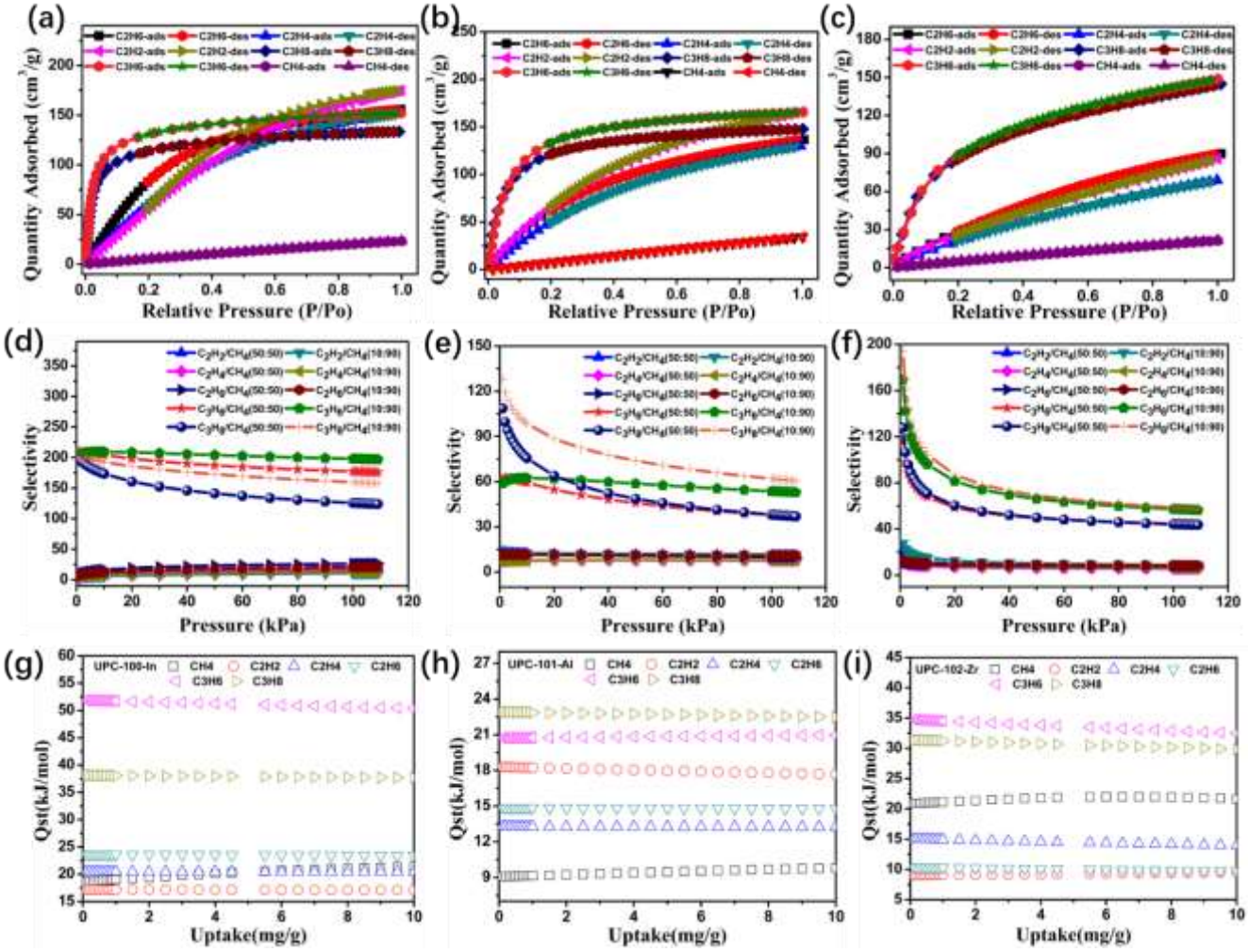

**Figure S10.** (a, b, and c) The $CH_4$, $C_2H_6$, $C_2H_4$, $C_2H_2$, $C_3H_8$ and $C_3H_6$ adsorption isotherms at 273 K for **UPC-100-In**, **UPC-101-Al**, and **UPC-102-Zr**; (d, e, and f) The $C_2H_6/CH_4$, $C_2H_4/CH_4$, $C_2H_2/CH_4$, $C_3H_8/CH_4$, and $C_3H_6/CH_4$ selectivity at 273 K for **UPC-100-In**, **UPC-101-Al**, and **UPC-102-Zr**, calculated by the ideal adsorbed solution theory (IAST) method (V/V: 50/50 and 10/90). (g, h, and i) The *Q*st for $CH_4$, $C_2H_6$, $C_2H_4$, $C_2H_2$, $C_3H_8$ and $C_3H_6$ for **UPC-100-In**, **UPC-101-Al**, and **UPC-102-Zr**.

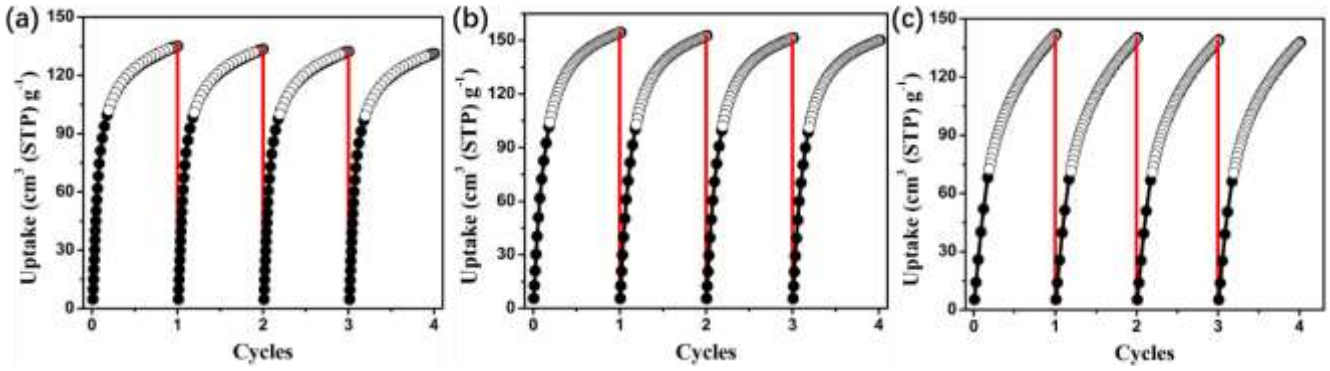


**Figure S11.** Cycles of $C_3H_6$ adsorption for **UPC-100-In (a)**, **UPC-101-Al (b)**, and **UPC-102-Zr (c)** at 298 K.

**Table S5.** Single component gas adsorption Data for **UPC-100-In.**

| Gas | T [K] | | Vads [$cm^3 \cdot g^{-1}$] | Amount [$mmol \cdot g^{-1}$] [wt%] | Qst [$KJ \cdot mol^{-1}$] |
|---|---|---|---|---|---|
| $CH_4$ | 273 | 23.3 | 1.04 | 1.66 | 18.7 |
| | 298 | 11.7 | 0.52 | 0.83 | |
| $C_2H_2$ | 273 | 174.9 | 7.81 | 20.30 | 17.2 |
| | 298 | 120.2 | 5.37 | 13.95 | |
| $C_2H_4$ | 273 | 151.8 | 6.78 | 18.97 | 20.5 |
| | 298 | 107.2 | 4.78 | 13.40 | |
| $C_2H_6$ | 273 | 155.9 | 6.96 | 20.88 | 23.6 |
| | 298 | 119.3 | 5.33 | 15.98 | |
| $C_3H_6$ | 273 | 152.0 | 6.75 | 28.37 | 51.9 |

| | | | | | |
|---|---|---|---|---|---|
| | 298 | 135.0 | 6.03 | 25.31 | |
| $C_3H_8$ | 273 | 133.5 | 5.96 | 23.84 | 38.1 |
| | 298 | 118.9 | 5.31 | 23.35 | |

**Table S6. UPC-100-In**: adsorption selectivity of hydrocarbon at 1 bar for different molar fraction of binary mixtures.

| binary gas mixtures | molar fraction | Selectivity (273 K) | Selectivity (298 K) |
|---|---|---|---|
| $C_2H_2/CH_4$ | 50:50 | 15.52 | 17.75 |
| | 10:90 | 11.09 | 12.44 |
| $C_2H_4/CH_4$ | 50:50 | 16.74 | 17.40 |
| | 10:90 | 13.04 | 12.83 |
| $C_2H_6/CH_4$ | 50:50 | 26.58 | 26.58 |
| | 10:90 | 21.05 | 17.90 |
| $C_3H_6/CH_4$ | 50:50 | 175.96 | 200.51 |
| | 10:90 | 196.91 | 115.29 |
| $C_3H_8/CH_4$ | 50:50 | 123.95 | 186.46 |
| | 10:90 | 157.96 | 134.39 |

**Table S7.** Single component gas adsorption Data for **UPC-101-Al.**

| Gas | T [K] | | Vads [$cm^3 \cdot g^{-1}$] | Amount [$mmol \cdot g^{-1}$] [wt%] | Qst [$KJ \cdot mol^{-1}$] |
|---|---|---|---|---|---|
| $CH_4$ | 273 | 34.3 | 1.53 | 2.45 | 9.1 |
| | 298 | 24.4 | 1.09 | 1.74 | |
| $C_2H_2$ | 273 | 166.0 | 7.41 | 19.27 | 18.3 |
| | 298 | 132.1 | 5.90 | 15.33 | |
| $C_2H_4$ | 273 | 129.8 | 5.79 | 16.22 | 13.3 |
| | 298 | 103.2 | 4.61 | 12.90 | |
| $C_2H_6$ | 273 | 136.6 | 6.10 | 18.3 | 14.9 |
| | 298 | 111.7 | 4.99 | 14.96 | |
| $C_3H_6$ | 273 | 165.6 | 7.39 | 31.05 | 20.7 |
| | 298 | 154.5 | 6.90 | 28.97 | |
| $C_3H_8$ | 273 | 147.7 | 6.59 | 29.00 | 22.9 |
| | 298 | 137.5 | 6.14 | 27.01 | |

**Table S8. UPC-101-Al**: adsorption selectivity of hydrocarbon at 1 bar for different molar fraction of binary mixtures.

| binary gas mixtures | molar fraction | Selectivity (273 K) | Selectivity (298 K) |
|---|---|---|---|
| $C_2H_2/CH_4$ | 50:50 | 10.86 | 9.24 |
| | 10:90 | 11.50 | 9.08 |
| $C_2H_4/CH_4$ | 50:50 | 7.45 | 6.88 |
| | 10:90 | 7.77 | 6.85 |
| $C_2H_6/CH_4$ | 50:50 | 9.82 | 8.95 |
| | 10:90 | 10.94 | 9.20 |
| $C_3H_6/CH_4$ | 50:50 | 36.92 | 32.50 |
| | 10:90 | 52.75 | 36.93 |
| $C_3H_8/CH_4$ | 50:50 | 36.83 | 37.25 |
| | 10:90 | 60.41 | 51.23 |

**Table S9. UPC-102-Zr**: adsorption selectivity of hydrocarbon at 1 bar for different molar fraction of binary mixtures.

| binary gas mixtures | molar fraction | Selectivity (273 K) | Selectivity (298 K) |
|---|---|---|---|
| $C_2H_2/CH_4$ | 50:50 | 7.41 | 12.09 |
| | 10:90 | 8.54 | 15.56 |
| $C_2H_4/CH_4$ | 50:50 | 5.65 | 8.52 |
| | 10:90 | 6.22 | 9.53 |
| $C_2H_6/CH_4$ | 50:50 | 8.09 | 13.06 |
| | 10:90 | 8.55 | 15.11 |
| $C_3H_6/CH_4$ | 50:50 | 44.14 | 44.04 |
| | 10:90 | 56.23 | 57.55 |
| $C_3H_8/CH_4$ | 50:50 | 43.59 | 42.53 |
| | 10:90 | 57.57 | 55.72 |

**Table S10.** Comparison of $H_2$ Adsorption Data for Selected MOFs.

| MOFs | $H_2$ uptake (77 K, 1bar, wt%) | ref | MOFs | $H_2$ uptake (77 K, 1bar, wt%) | ref |
|---|---|---|---|---|---|
| **UPC-100-In** | 1.56 | This work | TUDMOF-1 | 1.75 | 18 |
| **UPC-101-Al** | 2.69 | This work | PMOF-3 | 2.47 | 19 |
| **UPC-102-Zr** | 1.92 | This work | MOF-505 | 2.47 | 20 |
| NOTT-400 | 2.14 | 1 | NOTT-100 | 2.59 | 21 |
| NOTT-401 | 2.31 | 1 | NOTT-101 | 2.52 | 21,22 |
| CUK-1 | 1.6 | 2 | NOTT-102 | 2.24 | 21,22 |
| SNU-5 | 1.83 | 3 | NOTT-103 | 2.63 | 22 |
| SNU-6 | 1.68 | 4 | NOTT-105 | 2.52 | 22 |
| ZIF-8 | 1.27 | 5 | NOTT-106 | 2.29 | 22 |
| ZIF-11 | 1.35 | 5 | NOTT-107 | 2.26 | 22 |
| SNU-4 | 2.07 | 6 | NOTT-109 | 2.33 | 22 |
| MOF-646 | 1.75 | 7 | NOTT-110 | 2.64 | 23 |
| MOF-5 | 1.32 | 8 | NOTT-111 | 2.56 | 23 |
| IRMOF-9 | 1.17 | 9 | PCN-12 | 3.05 | 24 |
| IRMOF-2 | 1.21 | 9 | PCN-14 | 2.7 | 25 |
| MOF-177 | 1.25 | 8 | PCN-16 | 2.6 | 26 |
| IRMOF-6 | 1.48 | 9 | PCN-21 | 1.6 | 27 |
| IRMOF-3 | 1.42 | 9 | PCN-46 | 1.95 | 28 |
| IRMOF-11 | 1.62 | 8 | SNU-5 | 2.84 | 29 |
| IRMOF-8 | 1.50 | 8 | SNU-21S | 1.95 | 30 |
| SNU-1 | 1.90 | 10 | SNU-21H | 1.64 | 30 |
| IRMOF-13 | 1.73 | 9 | SNU-50’ | 2.1 | 31 |
| SNU-77H | 1.79 | 11 | UTSA-20 | 2.9 | 32 |
| IRMOF-20 | 1.35 | 9 | PCN-61 | 2.25 | 33 |
| FJI-1 | 1.02 | 12 | NOTT-119 | 1.4 | 34 |
| MOF-74(Mg) | 2.2 | 13 | PCN-69 | 1.7 | 35 |
| MOF-74(Zn) | 1.77 | 9 | PCN-66 | 1.79 | 33 |
| PCN-9 | 1.53 | 14 | PCN-68 | 1.87 | 33 |
| PCN-6 | 1.9 | 15 | NU-100 | 1.82 | 36 |
| PCN-6’ | 1.35 | 16 | PMOF-2(Cu) | 2.29 | 37 |
| UMCM-150 | 2.1 | 17 | NOTT-140 | 2.5 | 38 |

**Table S11.** Comparison of Light Hydrocarbon Adsorption Data for Selected MOFs.

| MOFs | T | $CH_4$ | $C_2H_2$ | $C_2H_4$ | $C_2H_6$ | $C_3H_6$ | $C_3H_8$ | ref |
|---|---|---|---|---|---|---|---|---|
| **UPC-100-In** | 273 | 23.3 | 174.9 | 151.8 | 155.9 | 152.0 | 133.5 | This work |
| | 298 | 11.7 | 120.2 | 107.2 | 119.3 | 135.0 | 118.9 | |
| **UPC-101-Al** | 273 | 34.3 | 166.0 | 129.8 | 136.6 | 165.6 | 147.7 | This work |
| | 298 | 24.4 | 132.1 | 103.2 | 111.7 | 154.5 | 137.5 | |
| **UPC-102-Zr** | 273 | 21.2 | 85.7 | 68.9 | 89.8 | 148.8 | 144.9 | This work |
| | 298 | 9.4 | 70.6 | 56.4 | 74.0 | 142.0 | 137.8 | |
| **UPC-33** | 273 | 9.7 | 65.1 | 43.6 | 51.8 | 114.2 | 111.8 | 29 |
| | 298 | 7.0 | 44.3 | 31.1 | 35.0 | 94.3 | 93.6 | |
| **FJI-C1** | 273 | | 135.9 | 85.2 | 123.6 | | 160.9 | 40 |
| | 298 | 9.7 | 93.8 | 64.0 | 87.4 | | 141.9 | |
| **FJI-C4** | 273 | 32.7 | 82.8 | 70.1 | 73.4 | | 74.7 | 41 |
| | 298 | 18.4 | 72.5 | 61.4 | 66.3 | | 71.5 | |
| **UTSA-33a** | 296 | 9.2mg/g | 97.1 | 76.2 | 83.0 | | | 42 |
| **1-mim** | 273 | 14.65 | 119.42 | 92.37 | 101.03 | | 102.92 | 43 |
| | 297 | 10.64 | 76.26 | 64.95 | 79.91 | | 96.87 | |
| **1-eim** | 273 | 19.32 | 117.84 | 87.30 | 99.348 | | 97.36 | 43 |
| | 297 | 11.48 | 73.70 | 61.29 | 75.38 | | 86.60 | |
| **1-pim** | 273 | 16.24 | 101.42 | 84.54 | 93.78 | | 97.31 | 43 |
| | 297 | 9.70 | 65.00 | 53.72 | 71.65 | | 83.29 | |
| **1-buim** | 273 | 14.08 | 93.54 | 73.16 | 81.77 | | 83.46 | 43 |
| | 297 | 8.86 | 56.14 | 48.70 | 63.00 | | 75.22 | |
| **UPC-21** | 273 | 43.2 | 196.5 | 123.1 | 137.6 | 124.1 | 116.2 | 44 |
| | 295 | 25.7 | 139.5 | 98.4 | 104.3 | 110.1 | 103.0 | |
| **SBMOF-1** | 298 | 18.85 | 30.44 | 30.0 | 29.5 | | | 45 |
| **SBMOF-2** | 298 | 17.3 | 64.7 | 59.8 | 62.2 | | | 45 |
| **ZJNU-51** | 278 | 22.7 | 131.5 | | | | | 46 |
| | 288 | 18.5 | 113.4 | | | | | |
| | 298 | 14.7 | 97.6 | | | | | |
| **ZJNU-81** | 278 | 33.2 | 250.0 | | | | | 47 |
| | 298 | 21.9 | 184.2 | | | | | |
| **ZJNU-82** | 278 | 33.2 | 248.7 | | | | | 47 |
| | 298 | 21.9 | 195.4 | | | | | |
| **ZJNU-83** | 278 | 33.9 | 241.3 | | | | | 47 |
| | 298 | 23.0 | 196.7 | | | | | |
| **BUT-52** | 273 | 13.2 | 86.7 | 56.9 | 71.6 | | | 48 |
| | 298 | 7.7 | 71.6 | 37.9 | 40.7 | | | |
| **UTSA-10a** | 296 | 5.8 | 43.0 | 31.0 | 48.5 | | | 49 |
| **M'MOF-20** | 195 | 70 | 268 | 81 | 77 | | 39 | 50 |
| | 273 | | 95.0 | 53.0 | | | 43.0 | |
| | 298 | 8.0 | 81.0 | 44.0 | 49.0 | | 47.0 | |

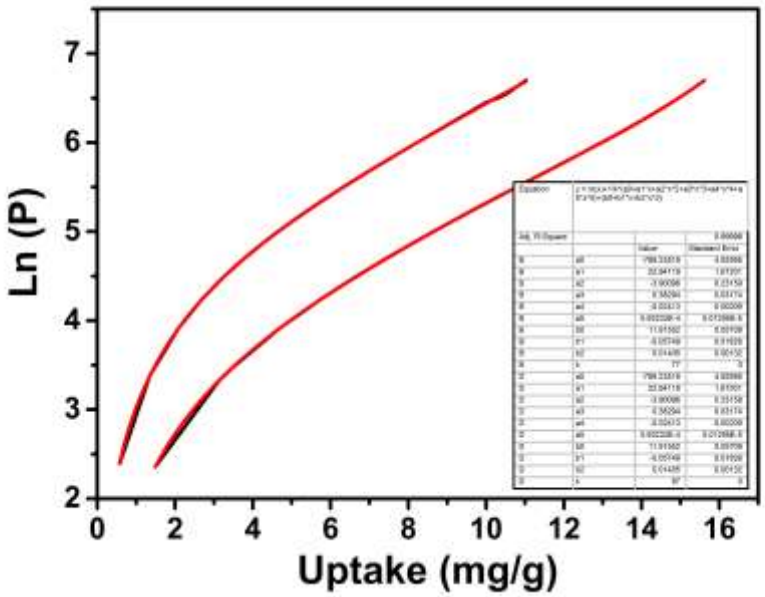


**Figure S12. UPC-100-In**: the parameters and optimized adsorption isotherms for calculated $Q_{st}$ of $H_2$ using a variant of the Clausius-Clapeyron equation.

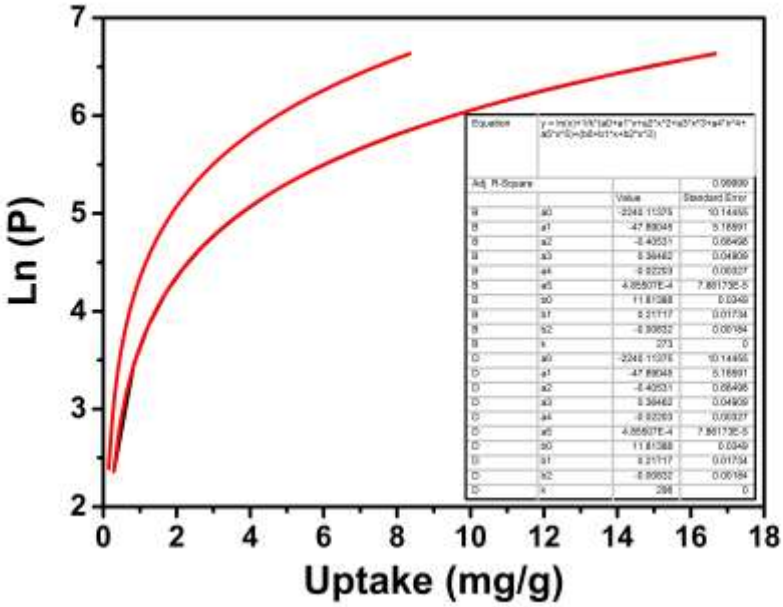


**Figure S13. UPC-100-In**: the parameters and optimized adsorption isotherms for calculated $Q_{st}$ of $CH_4$ using a variant of the Clausius-Clapeyron equation.

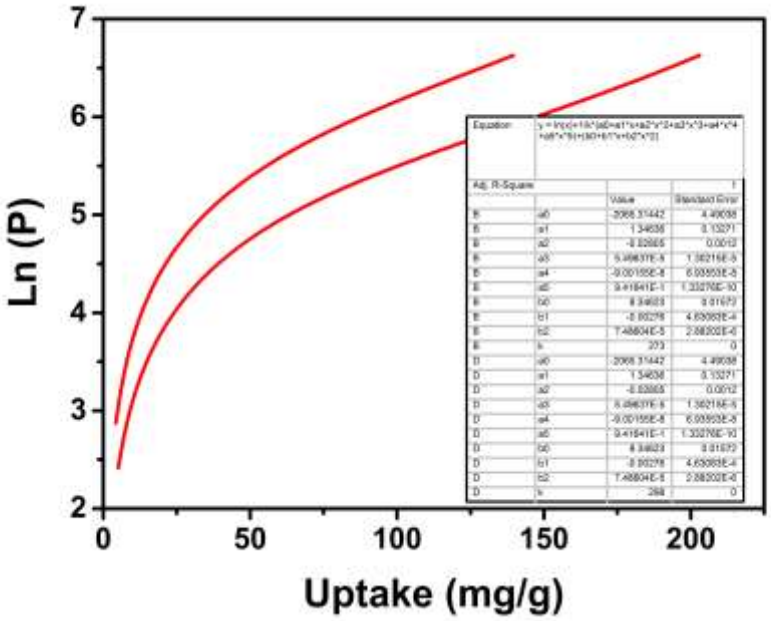


**Figure S14. UPC-100-In**: the parameters and optimized adsorption isotherms for calculated $Q_{st}$ of $C_2H_2$ using a variant of the Clausius-Clapeyron equation.

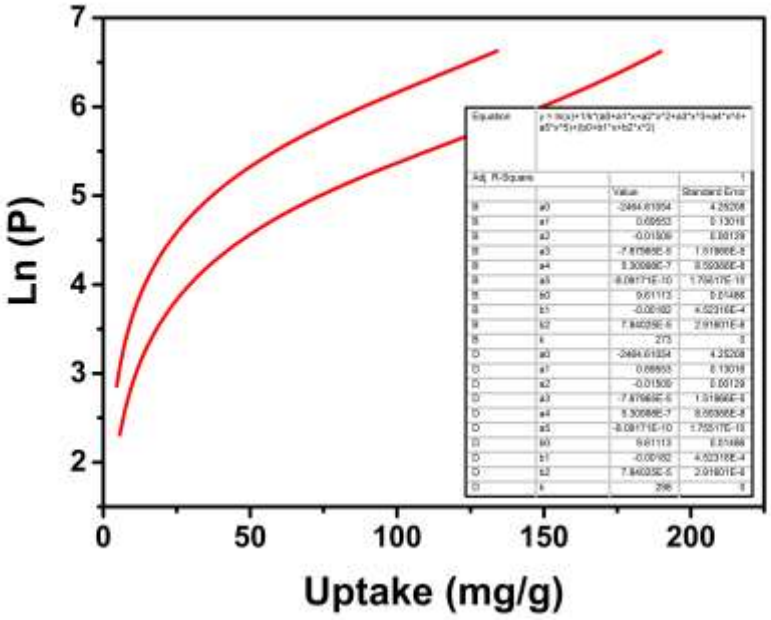


**Figure S15. UPC-100-In**: the parameters and optimized adsorption isotherms for calculated $Q_{st}$ of $C_2H_4$ using a variant of the Clausius-Clapeyron equation.

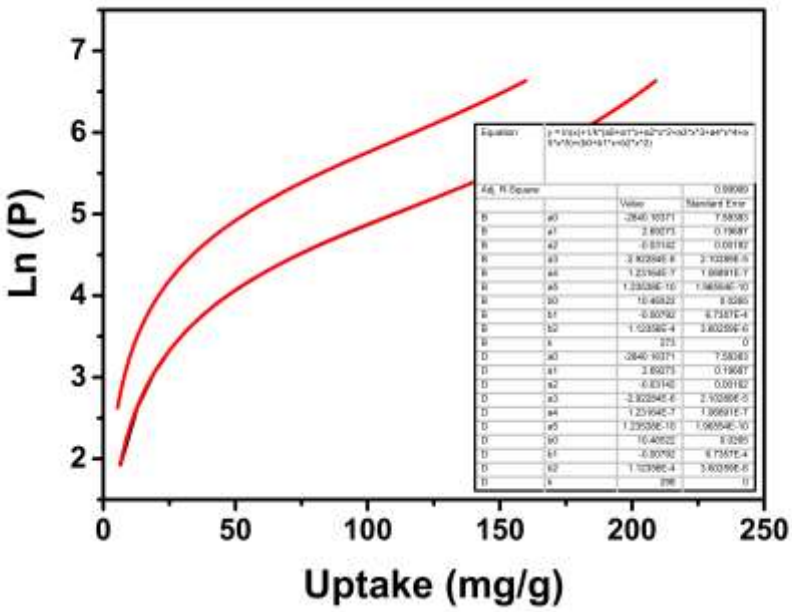


**Figure S16. UPC-100-In**: the parameters and optimized adsorption isotherms for calculated $Q_{st}$ of $C_2H_6$ using a variant of the Clausius-Clapeyron equation.

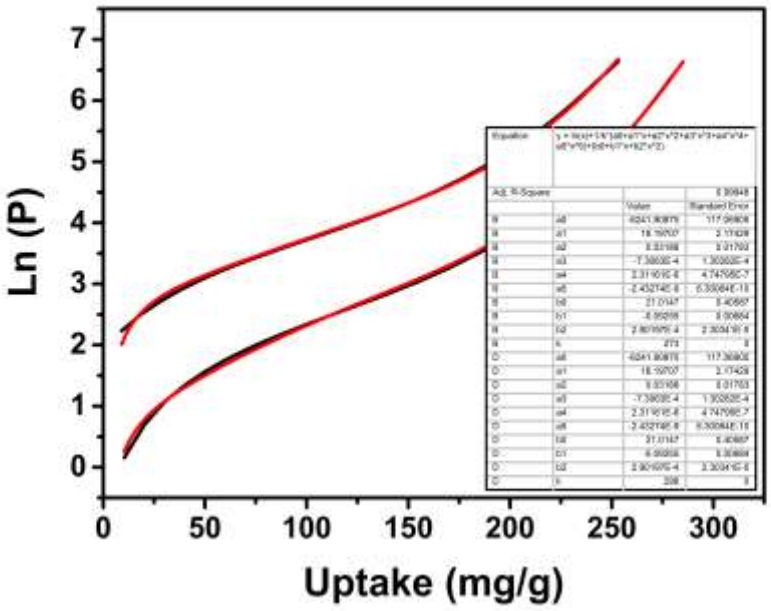


**Figure S17. UPC-100-In**: the parameters and optimized adsorption isotherms for calculated $Q_{st}$ of $C_3H_6$ using a variant of the Clausius-Clapeyron equation.

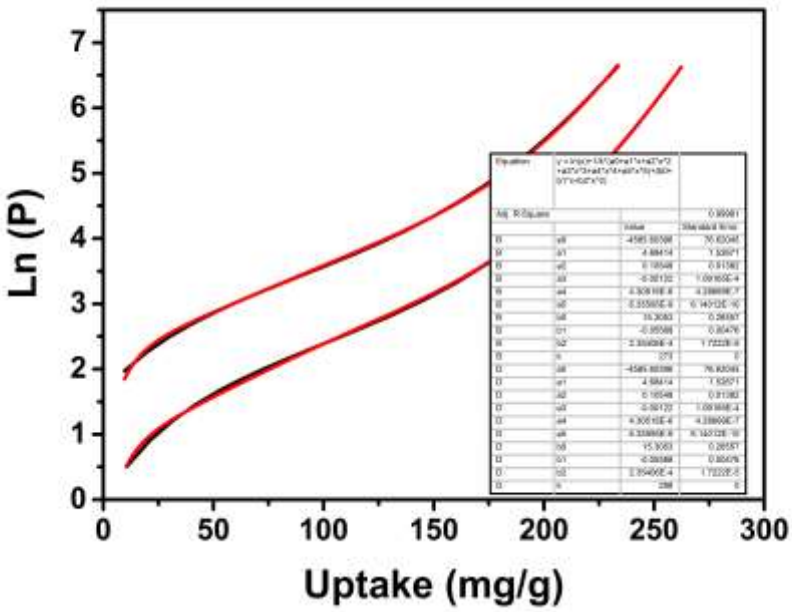


**Figure S18. UPC-100-In**: the parameters and optimized adsorption isotherms for calculated $Q_{st}$ of $C_3H_8$ using a variant of the Clausius-Clapeyron equation.

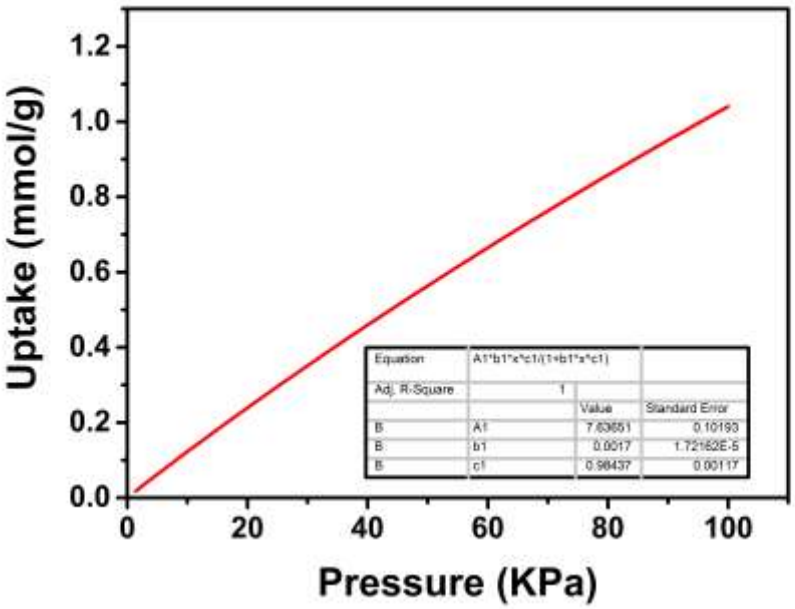


**Figure S19. UPC-100-In**: the parameters and optimized adsorption isotherms of $CH_4$ for calculated selectivity by using Ideal Adsorbed Solution Theory (IAST) at 273 K.

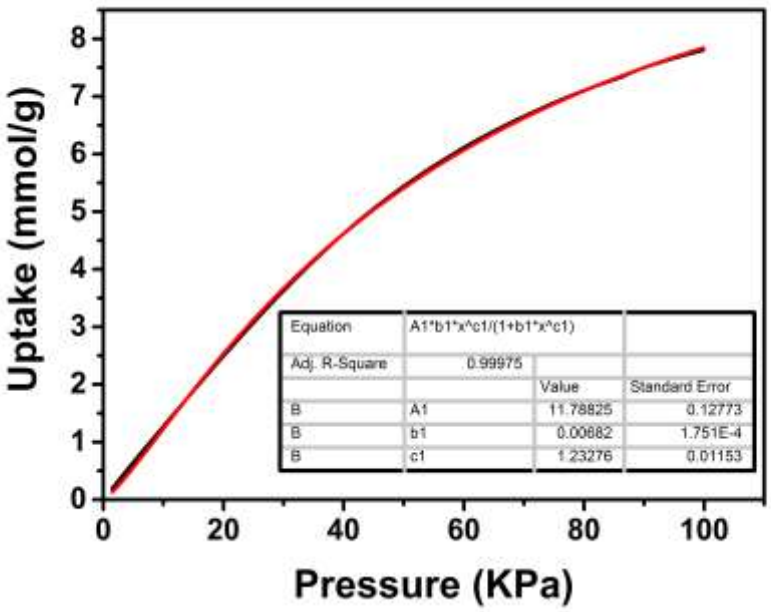


**Figure S20. UPC-100-In**: the parameters and optimized adsorption isotherms of $C_2H_2$ for calculated selectivity by using Ideal Adsorbed Solution Theory (IAST) at 273 K.

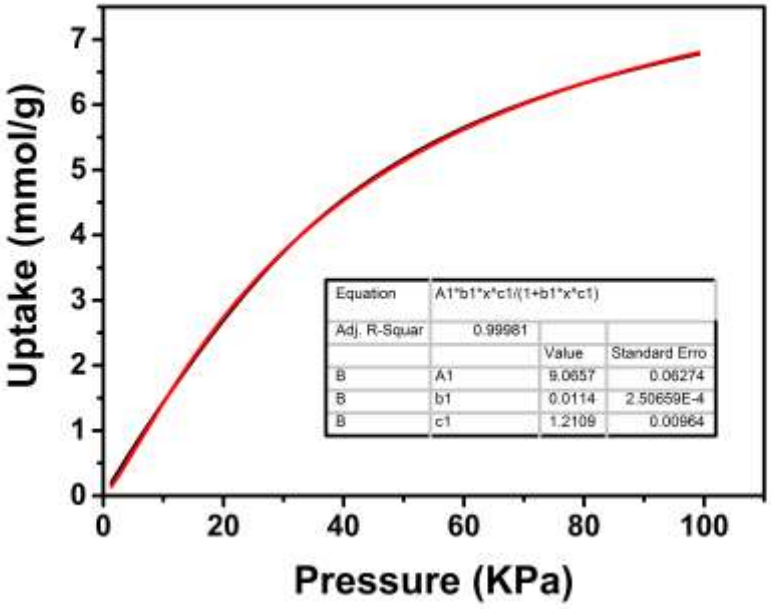


**Figure S21. UPC-100-In**: the parameters and optimized adsorption isotherms of $C_2H_4$ for calculated selectivity by using Ideal Adsorbed Solution Theory (IAST) at 273 K.

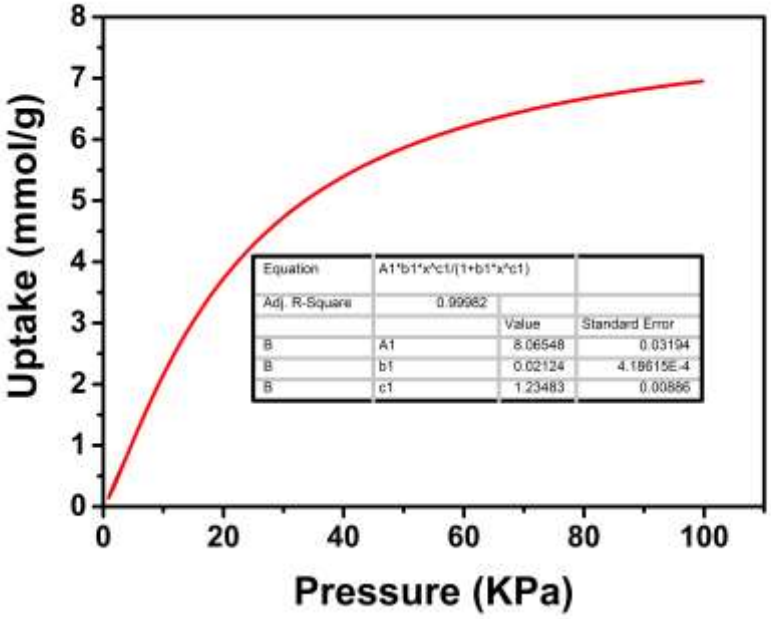


**Figure S22. UPC-100-In**: the parameters and optimized adsorption isotherms of $C_2H_6$ for calculated selectivity by using Ideal Adsorbed Solution Theory (IAST) at 273 K.

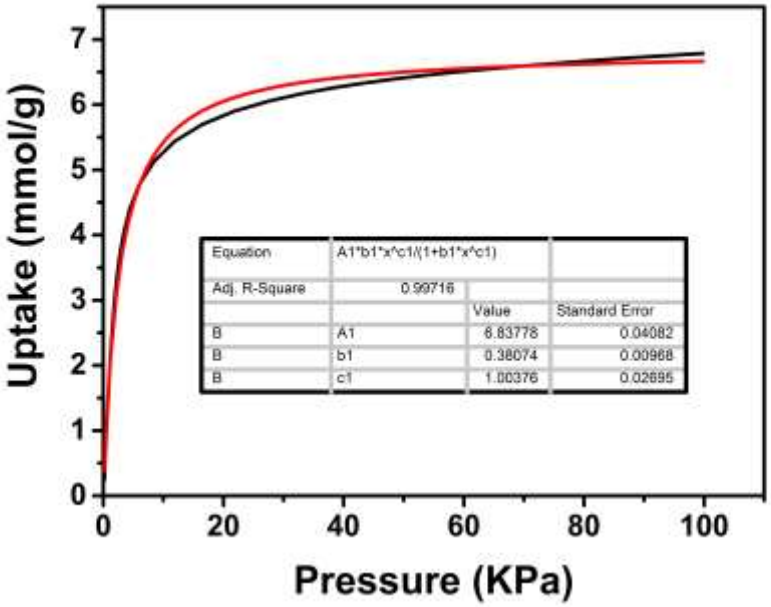


**Figure S23. UPC-100-In**: the parameters and optimized adsorption isotherms of $C_3H_6$ for calculated selectivity by using Ideal Adsorbed Solution Theory (IAST) at 273 K.

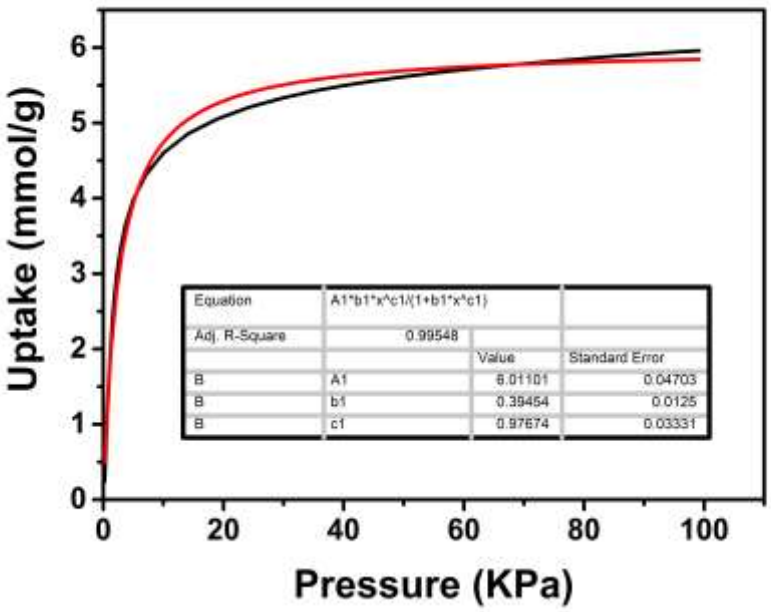


**Figure S24. UPC-100-In**: the parameters and optimized adsorption isotherms of $C_3H_8$ for calculated selectivity by using Ideal Adsorbed Solution Theory (IAST) at 273 K.

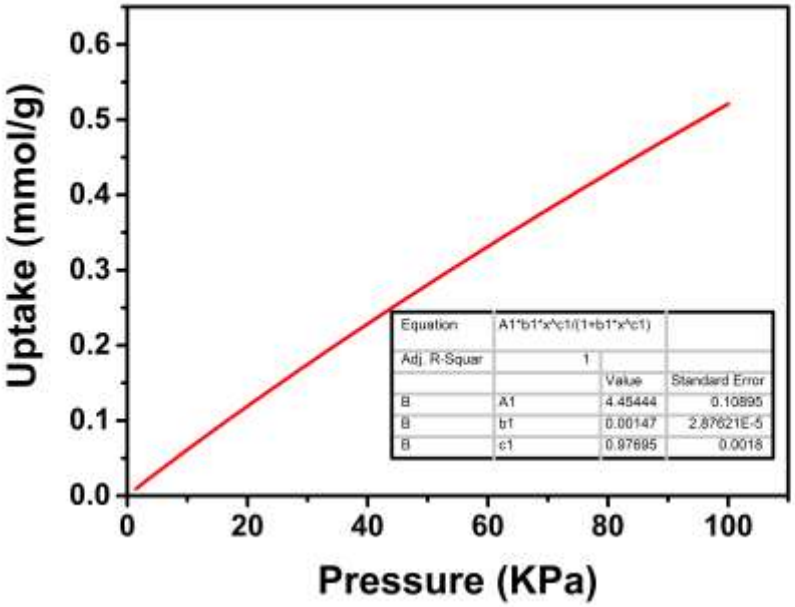


**Figure S25. UPC-100-In**: the parameters and optimized adsorption isotherms of $CH_4$ for calculated selectivity by using Ideal Adsorbed Solution Theory (IAST) at 298 K.

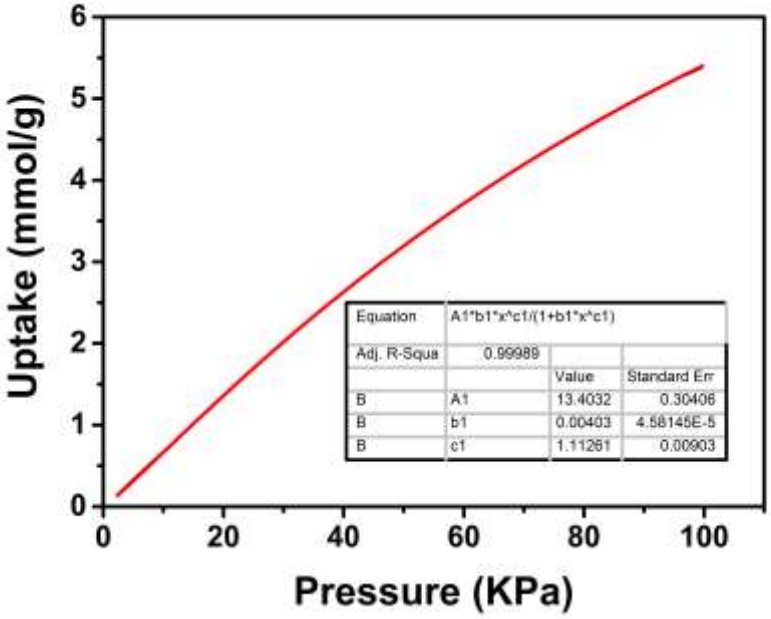


**Figure S26. UPC-100-In**: the parameters and optimized adsorption isotherms of $C_2H_2$ for calculated selectivity by using Ideal Adsorbed Solution Theory (IAST) at 298 K.

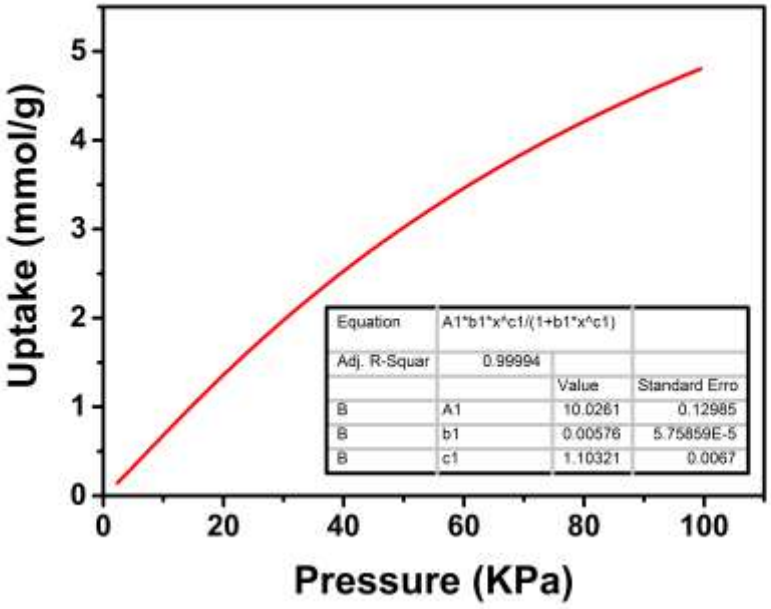


**Figure S27. UPC-100-In**: the parameters and optimized adsorption isotherms of $C_2H_4$ for calculated selectivity by using Ideal Adsorbed Solution Theory (IAST) at 298 K.

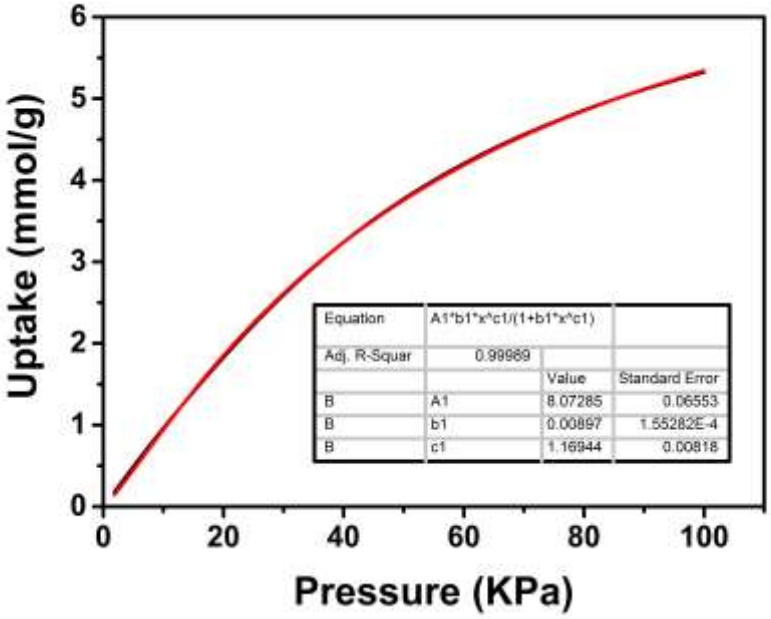


**Figure S28. UPC-100-In**: the parameters and optimized adsorption isotherms of $C_2H_6$ for calculated selectivity by using Ideal Adsorbed Solution Theory (IAST) at 298 K.

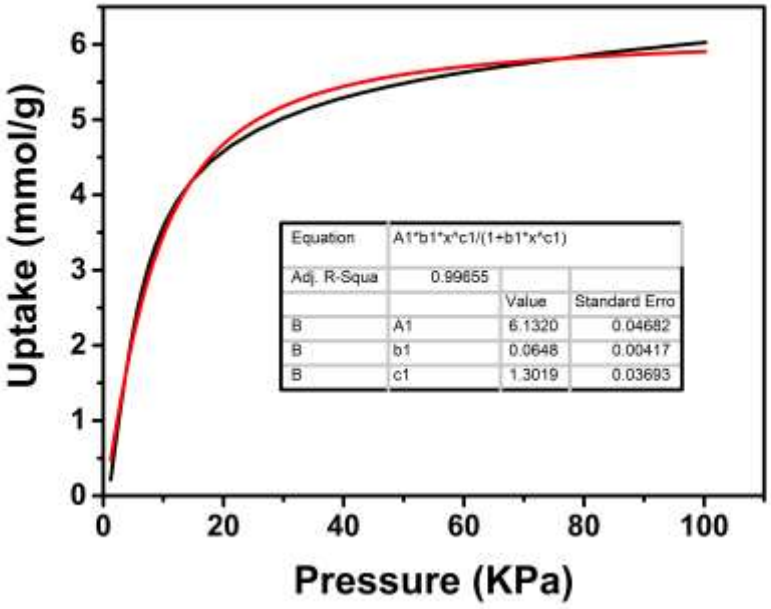


**Figure S29. UPC-100-In**: the parameters and optimized adsorption isotherms of $C_3H_6$ for calculated selectivity by using Ideal Adsorbed Solution Theory (IAST) at 298 K.

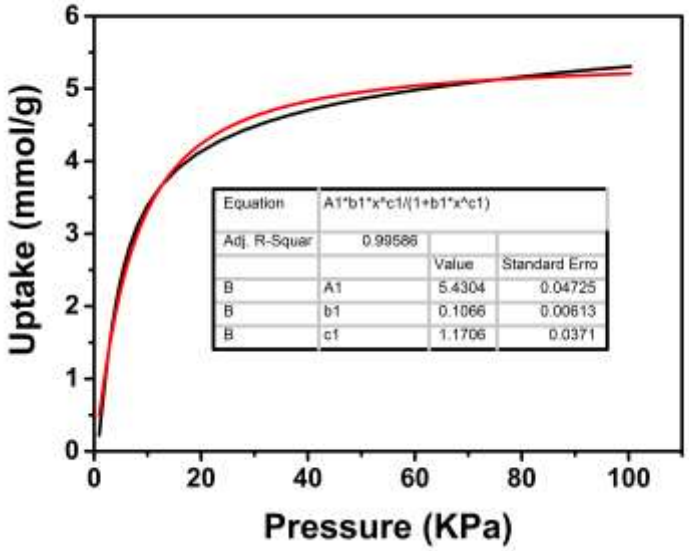


**Figure S30. UPC-100-In**: the parameters and optimized adsorption isotherms of $C_3H_8$ for calculated selectivity by using Ideal Adsorbed Solution Theory (IAST) at 298 K.

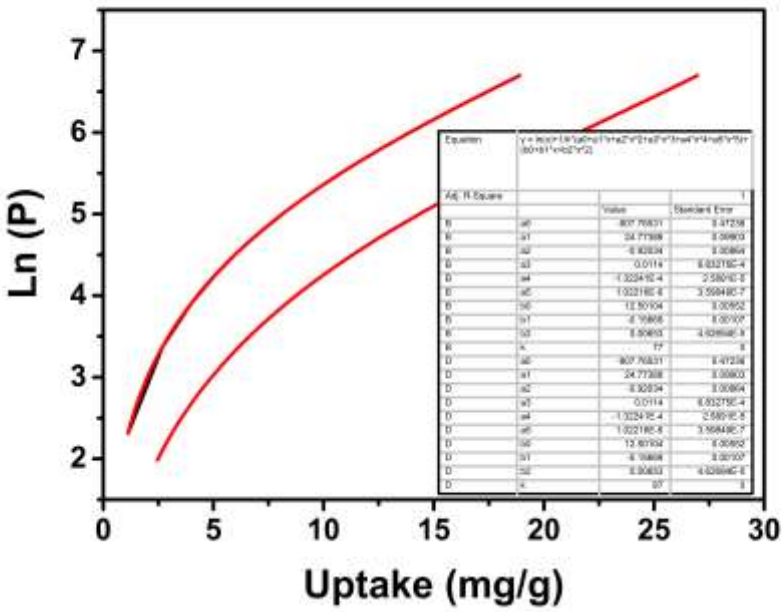


**Figure S31. UPC-101-Al**: the parameters and optimized adsorption isotherms for calculated $Q_{st}$ of $H_2$ using a variant of the Clausius-Clapeyron equation.

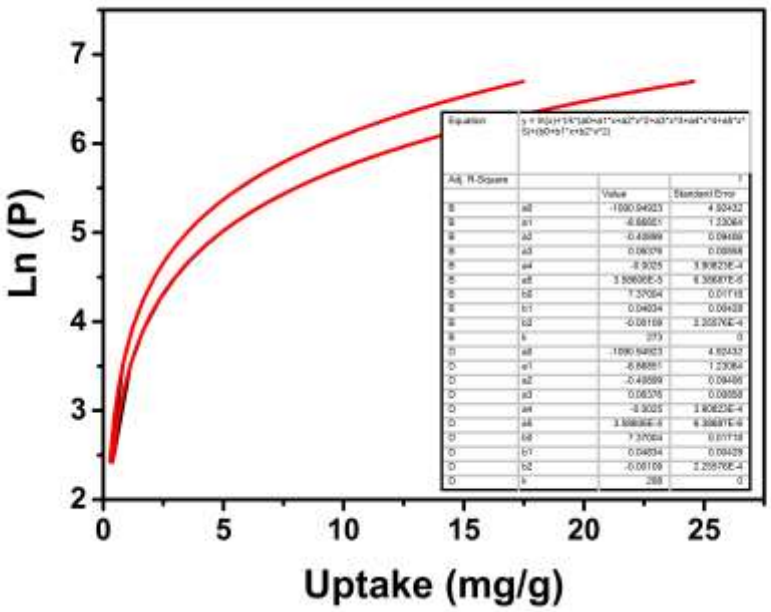


**Figure S32. UPC-101-Al**: the parameters and optimized adsorption isotherms for calculated $Q_{st}$ of $CH_4$ using a variant of the Clausius-Clapeyron equation.

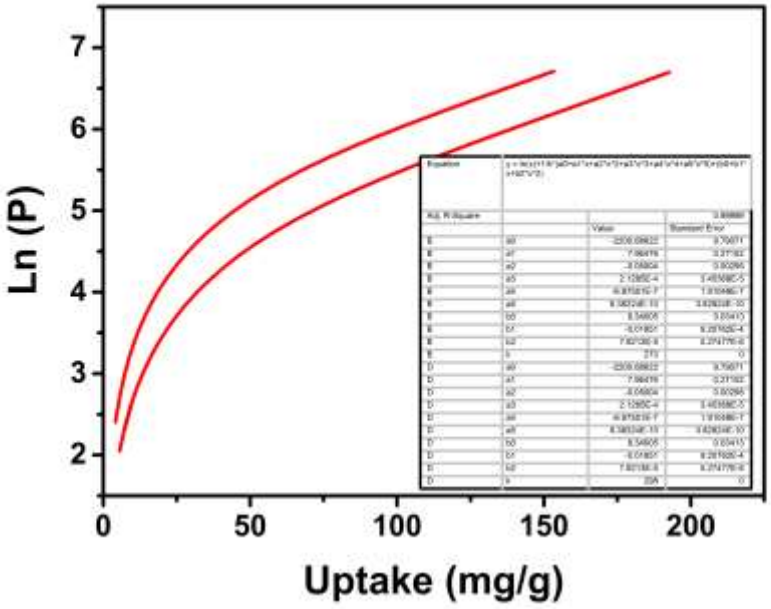


**Figure S33. UPC-101-Al**: the parameters and optimized adsorption isotherms for calculated $Q_{st}$ of $C_2H_2$ using a variant of the Clausius-Clapeyron equation.

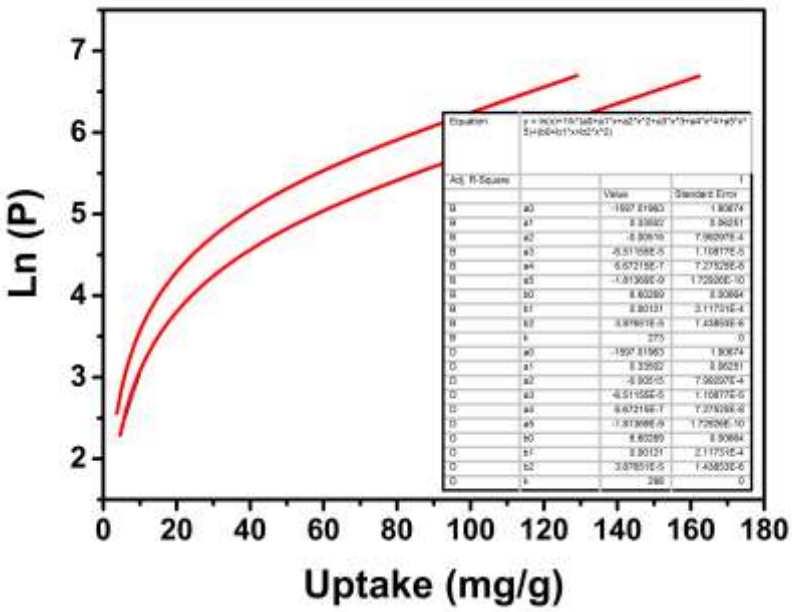


**Figure S34. UPC-101-Al**: the parameters and optimized adsorption isotherms for calculated $Q_{st}$ of $C_2H_4$ using a variant of the Clausius-Clapeyron equation.

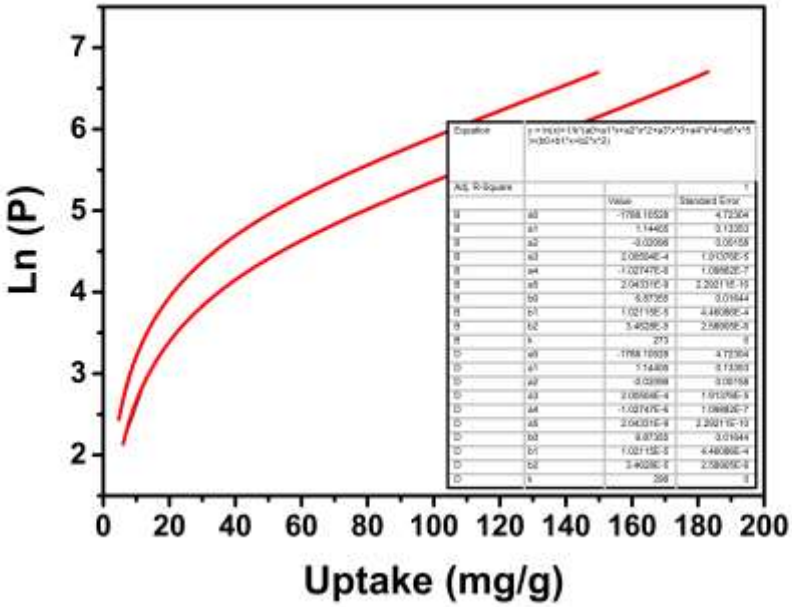


**Figure S35. UPC-101-Al**: the parameters and optimized adsorption isotherms for calculated $Q_{st}$ of $C_2H_6$ using a variant of the Clausius-Clapeyron equation.

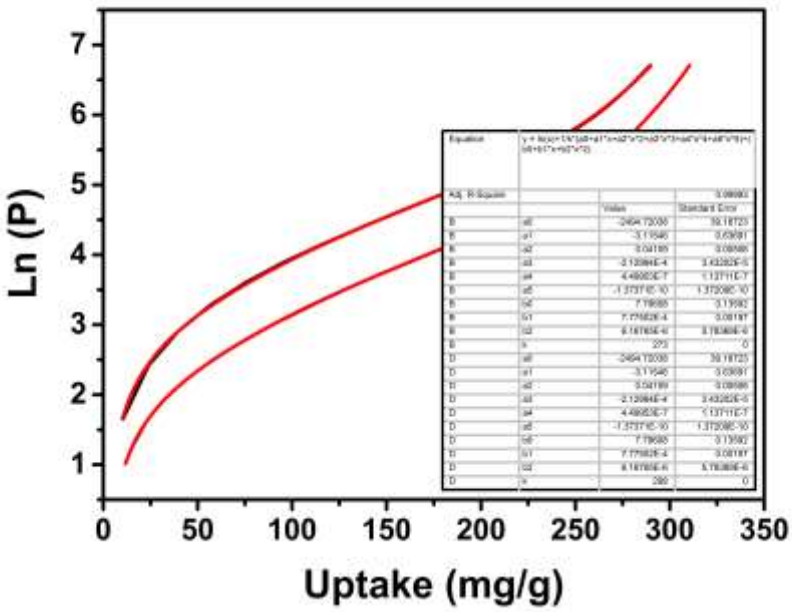


**Figure S36. UPC-101-Al**: the parameters and optimized adsorption isotherms for calculated $Q_{st}$ of $C_3H_6$ using a variant of the Clausius-Clapeyron equation.

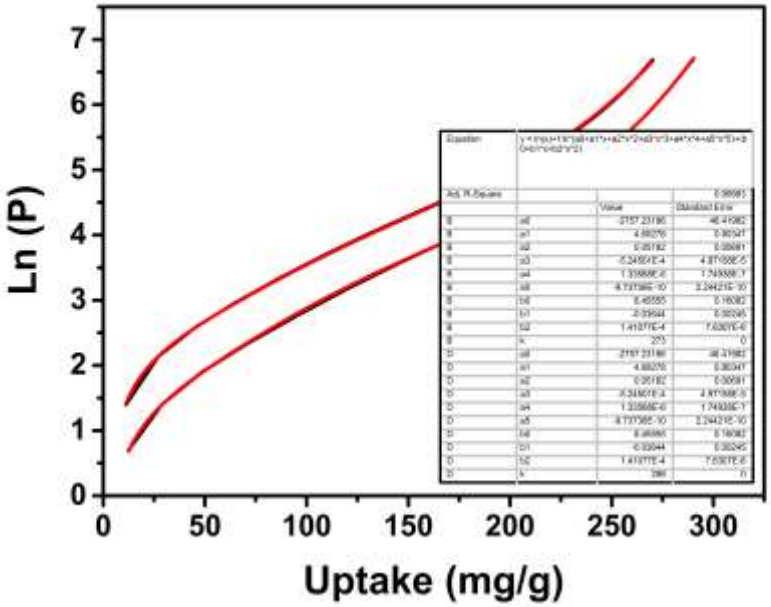


**Figure S37. UPC-101-Al**: the parameters and optimized adsorption isotherms for calculated $Q_{st}$ of $C_3H_8$ using a variant of the Clausius-Clapeyron equation.

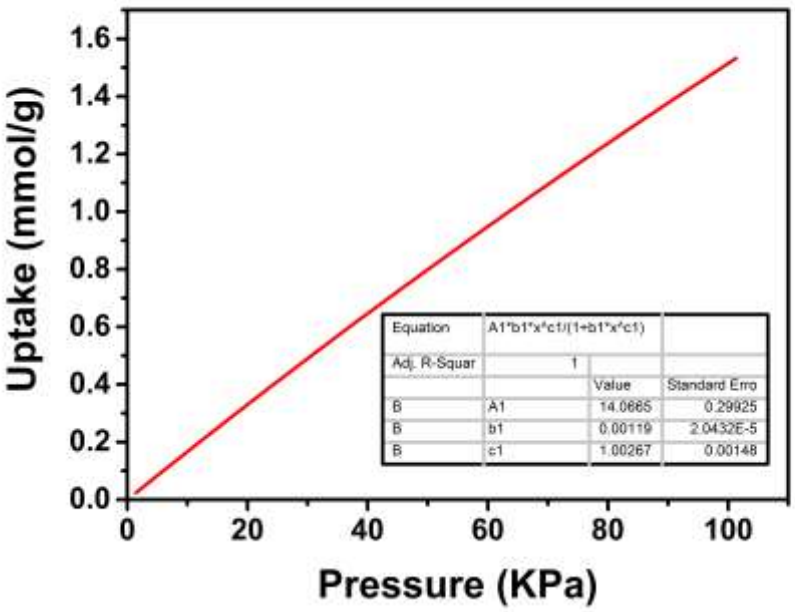


**Figure S38. UPC-101-Al**: the parameters and optimized adsorption isotherms of $CH_4$ for calculated selectivity by using Ideal Adsorbed Solution Theory (IAST) at 273 K.

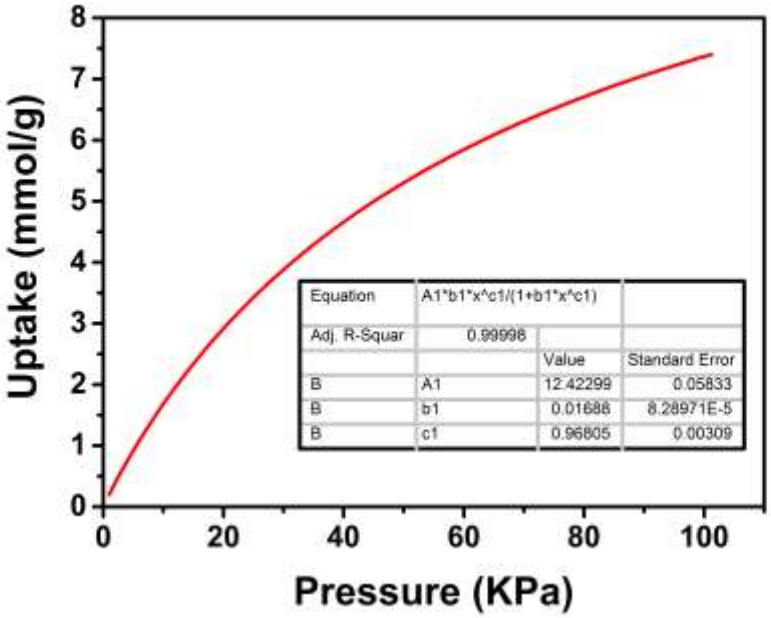


**Figure S39. UPC-101-Al**: the parameters and optimized adsorption isotherms of $C_2H_2$ for calculated selectivity by using Ideal Adsorbed Solution Theory (IAST) at 273 K.

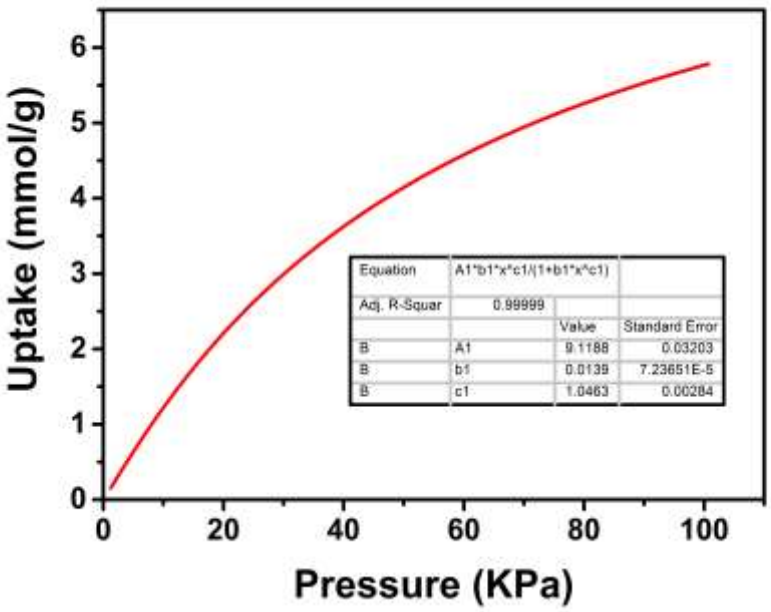


**Figure S40. UPC-101-Al**: the parameters and optimized adsorption isotherms of $C_2H_4$ for calculated selectivity by using Ideal Adsorbed Solution Theory (IAST) at 273 K.

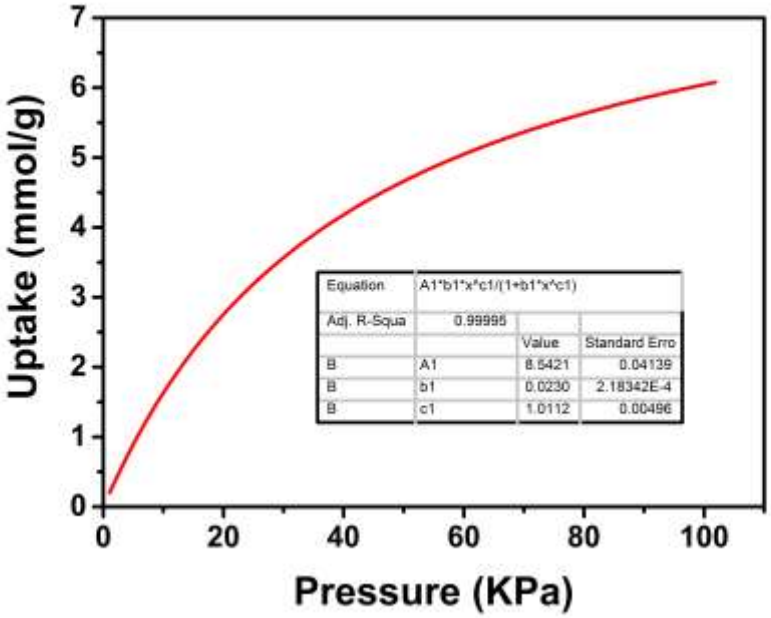


**Figure S41. UPC-101-Al**: the parameters and optimized adsorption isotherms of $C_2H_6$ for calculated selectivity by using Ideal Adsorbed Solution Theory (IAST) at 273 K.

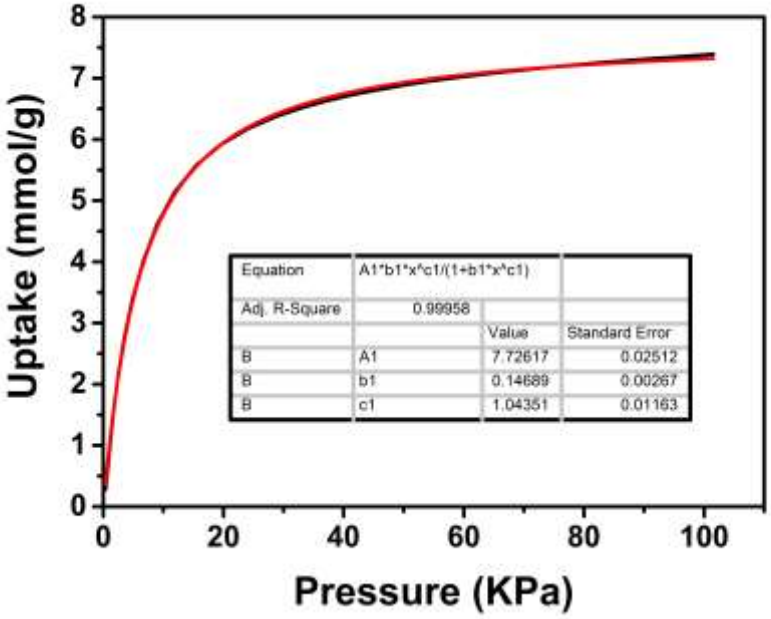


**Figure S42. UPC-101-Al**: the parameters and optimized adsorption isotherms of $C_3H_6$ for calculated selectivity by using Ideal Adsorbed Solution Theory (IAST) at 273 K.

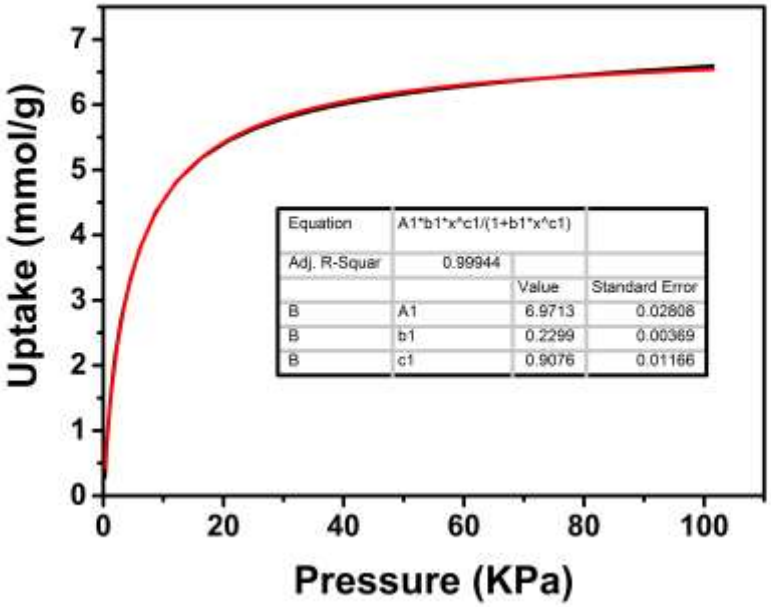


**Figure S43. UPC-101-Al**: the parameters and optimized adsorption isotherms of $C_3H_8$ for calculated selectivity by using Ideal Adsorbed Solution Theory (IAST) at 273 K.

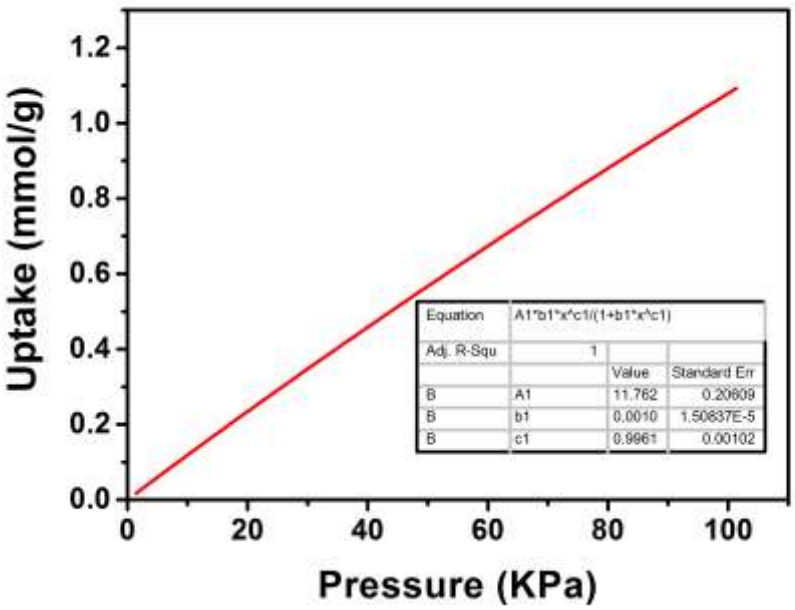


**Figure S44. UPC-101-Al**: the parameters and optimized adsorption isotherms of $CH_4$ for calculated selectivity by using Ideal Adsorbed Solution Theory (IAST) at 298 K.

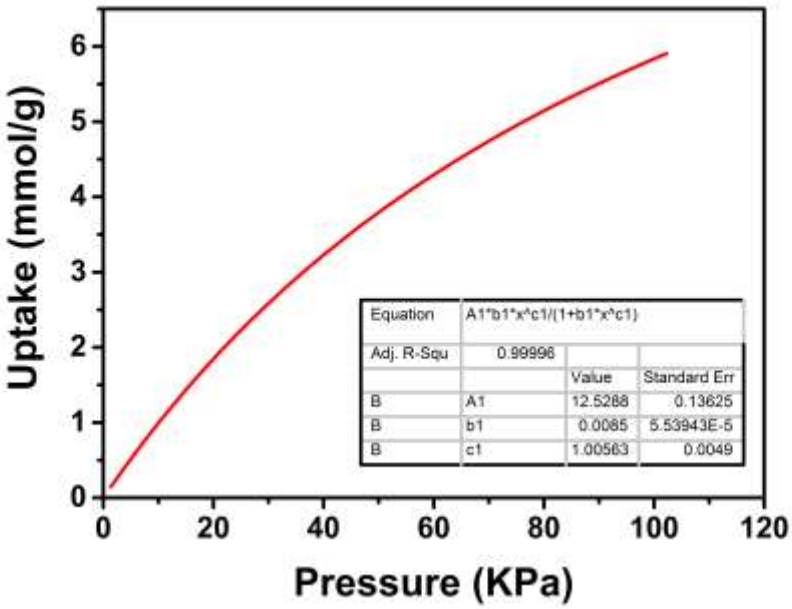


**Figure S45. UPC-101-Al**: the parameters and optimized adsorption isotherms of $C_2H_2$ for calculated selectivity by using Ideal Adsorbed Solution Theory (IAST) at 298 K.

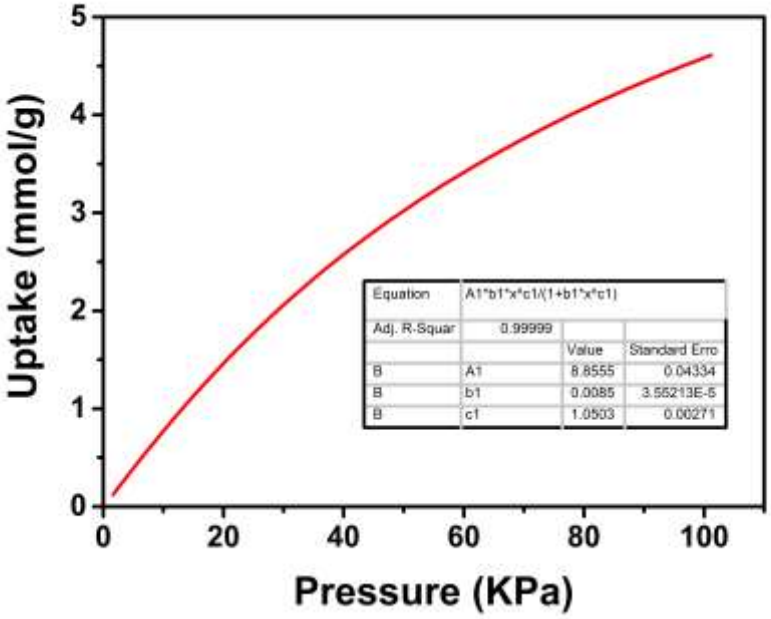


**Figure S46. UPC-101-Al**: the parameters and optimized adsorption isotherms of $C_2H_4$ for calculated selectivity by using Ideal Adsorbed Solution Theory (IAST) at 298 K.

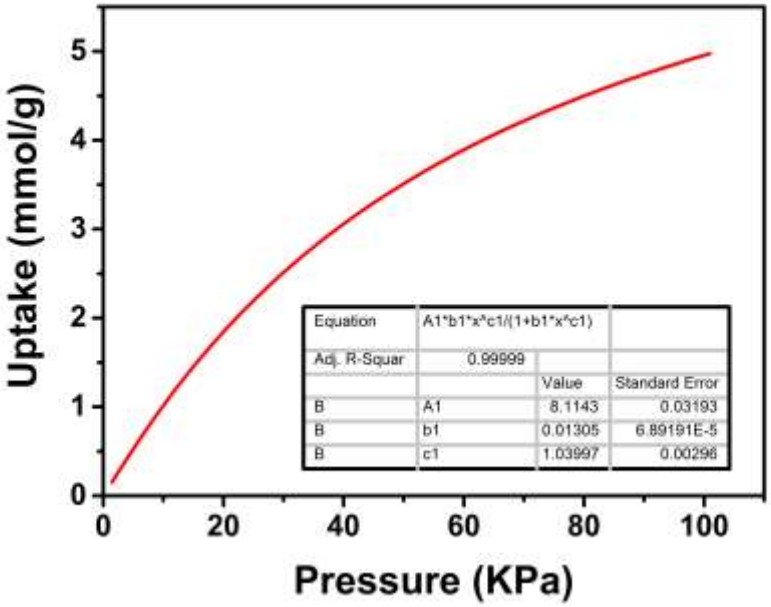


**Figure S47. UPC-101-Al**: the parameters and optimized adsorption isotherms of $C_2H_6$ for calculated selectivity by using Ideal Adsorbed Solution Theory (IAST) at 298 K.

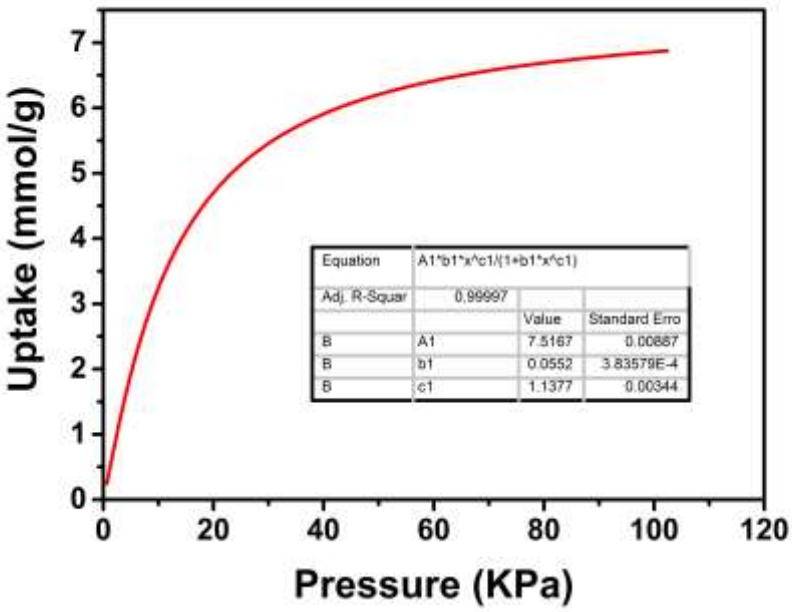


**Figure S48. UPC-101-Al**: the parameters and optimized adsorption isotherms of $C_3H_6$ for calculated selectivity by using Ideal Adsorbed Solution Theory (IAST) at 298 K.

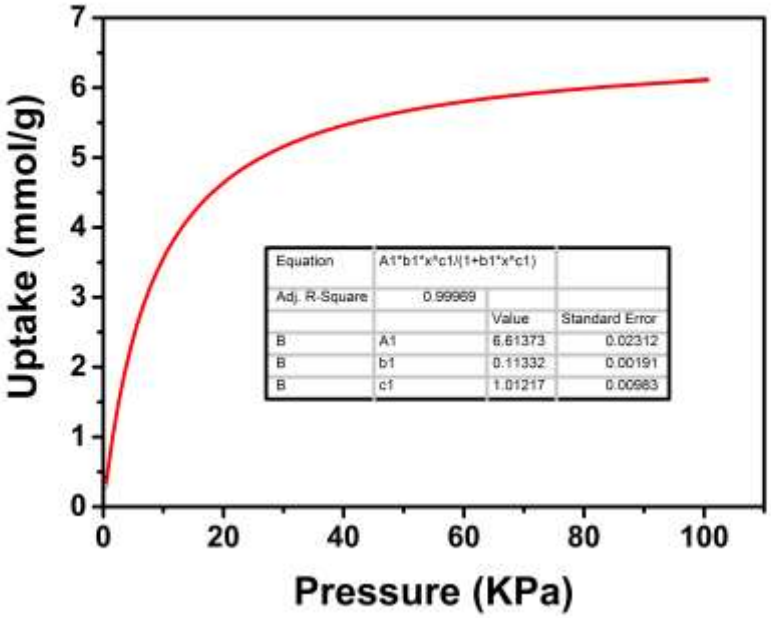


**Figure S49. UPC-101-Al**: the parameters and optimized adsorption isotherms of $C_3H_8$ for calculated selectivity by using Ideal Adsorbed Solution Theory (IAST) at 298 K.

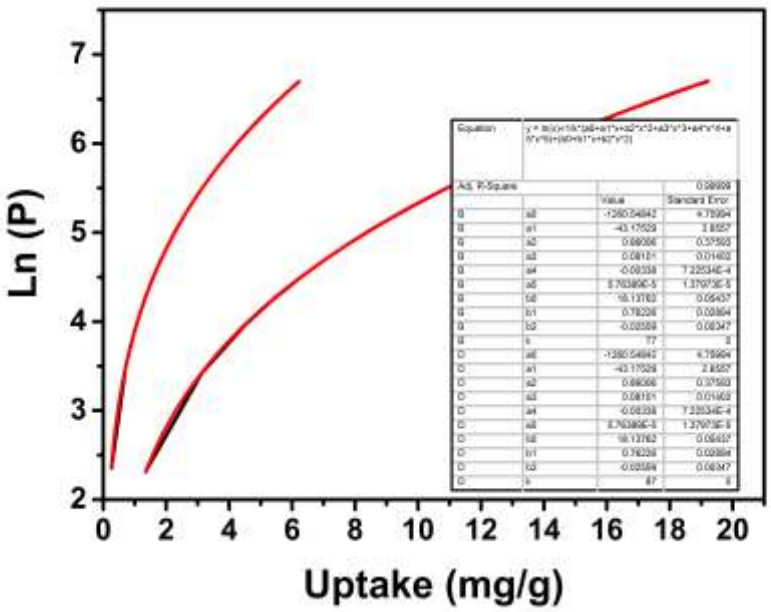


**Figure S50. UPC-102-Zr**: the parameters and optimized adsorption isotherms for calculated $Q_{st}$ of $H_2$ using a variant of the Clausius-Clapeyron equation.

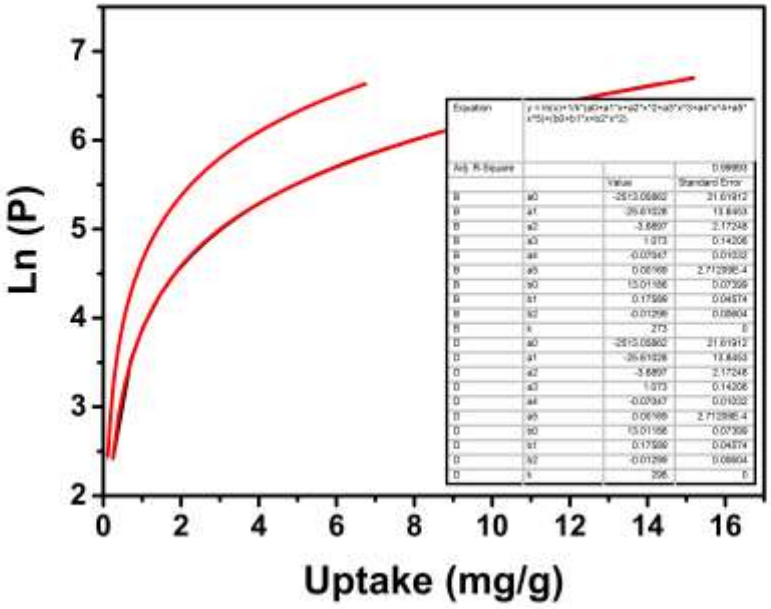


**Figure S51. UPC-102-Zr**: the parameters and optimized adsorption isotherms for calculated $Q_{st}$ of $CH_4$ using a variant of the Clausius-Clapeyron equation.

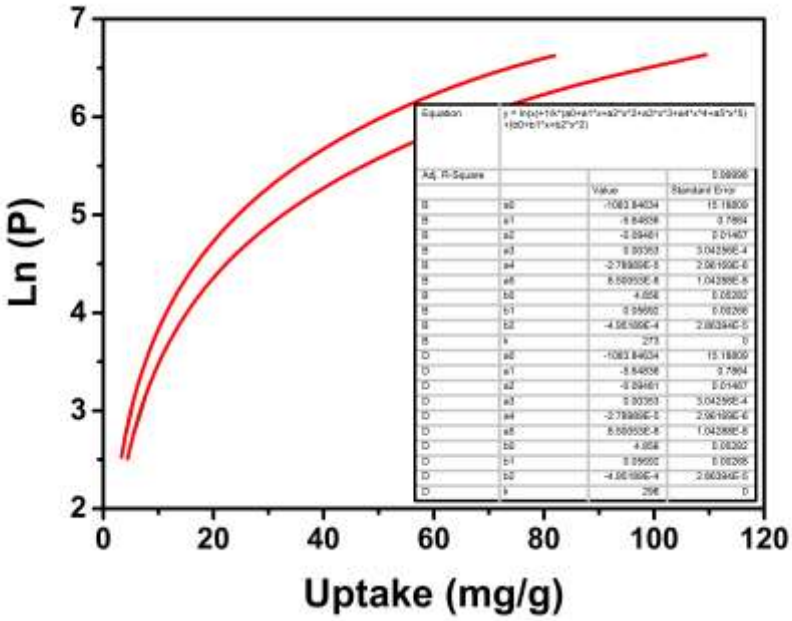


**Figure S52. UPC-102-Zr**: the parameters and optimized adsorption isotherms for calculated $Q_{st}$ of $C_2H_2$ using a variant of the Clausius-Clapeyron equation.

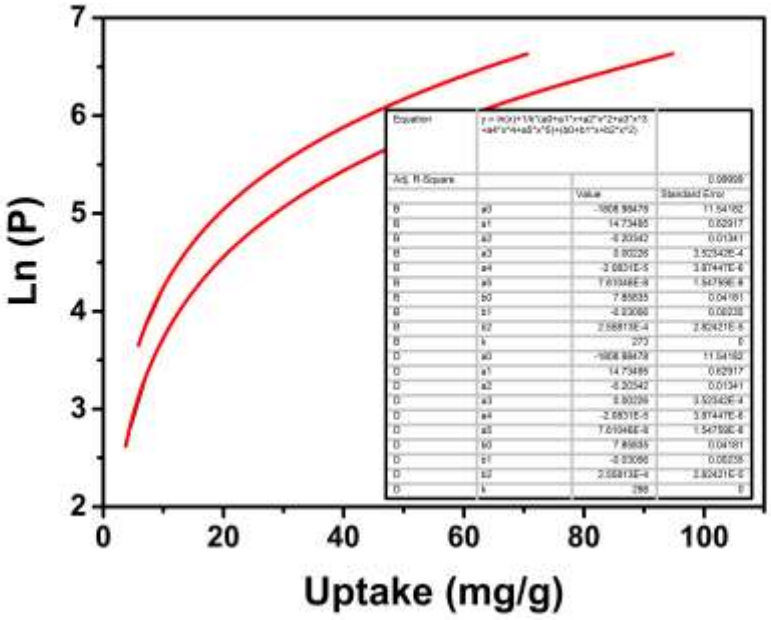


**Figure S53. UPC-102-Zr**: the parameters and optimized adsorption isotherms for calculated $Q_{st}$ of $C_2H_4$ using a variant of the Clausius-Clapeyron equation.

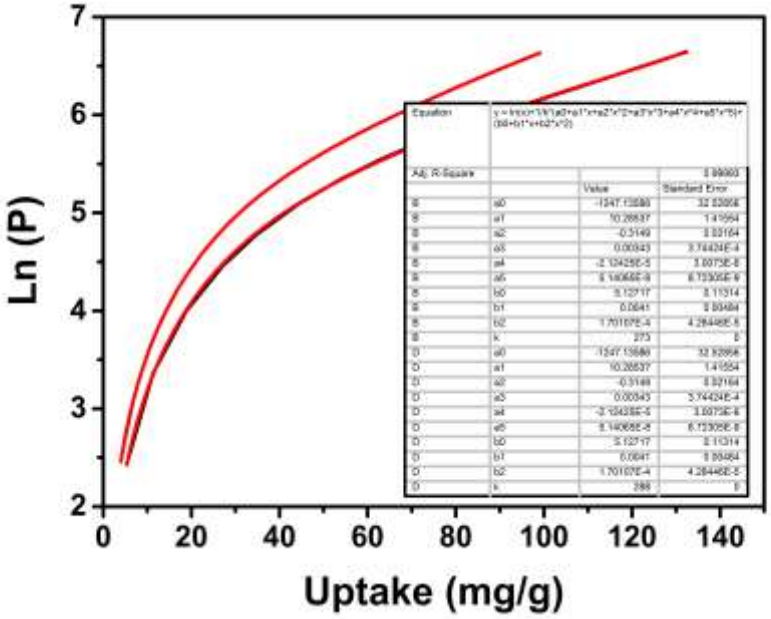


**Figure S54. UPC-102-Zr**: the parameters and optimized adsorption isotherms for calculated $Q_{st}$ of $C_2H_6$ using a variant of the Clausius-Clapeyron equation.

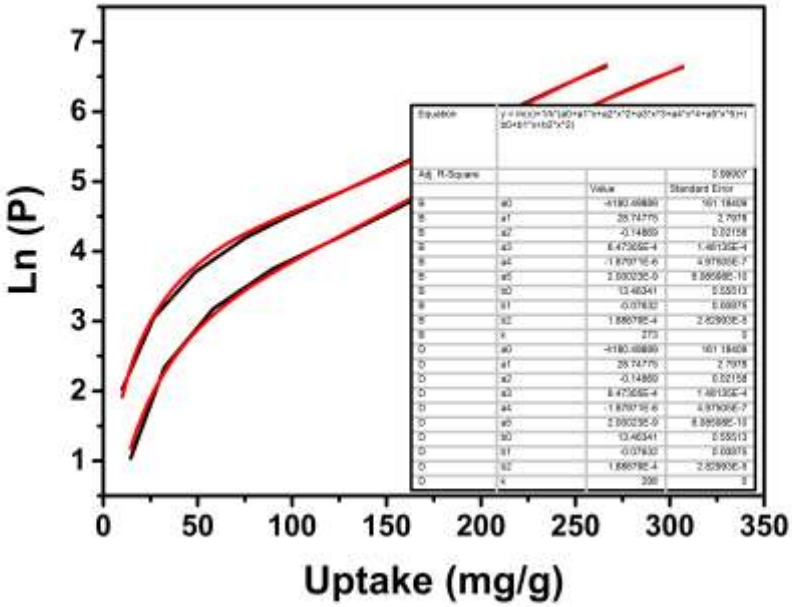


**Figure S55. UPC-102-Zr**: the parameters and optimized adsorption isotherms for calculated $Q_{st}$ of $C_3H_6$ using a variant of the Clausius-Clapeyron equation.

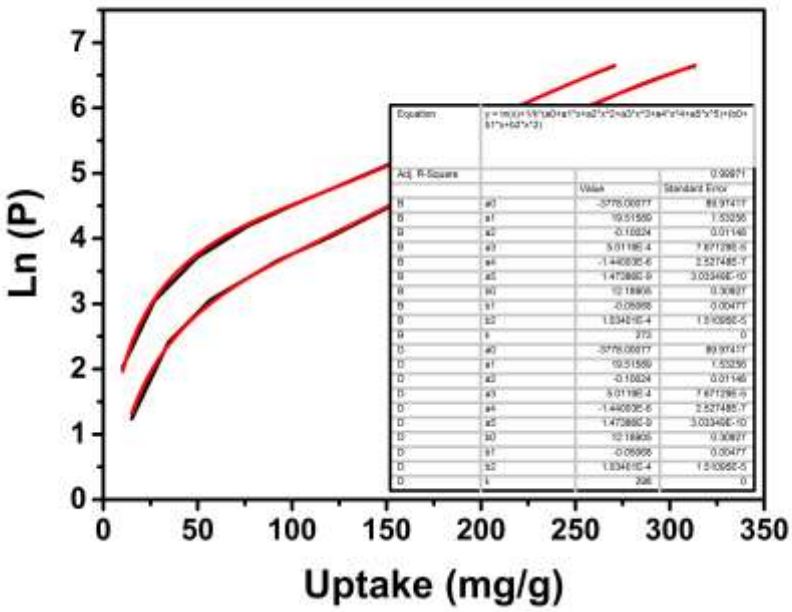


**Figure S56. UPC-102-Zr**: the parameters and optimized adsorption isotherms for calculated $Q_{st}$ of $C_3H_8$ using a variant of the Clausius-Clapeyron equation.

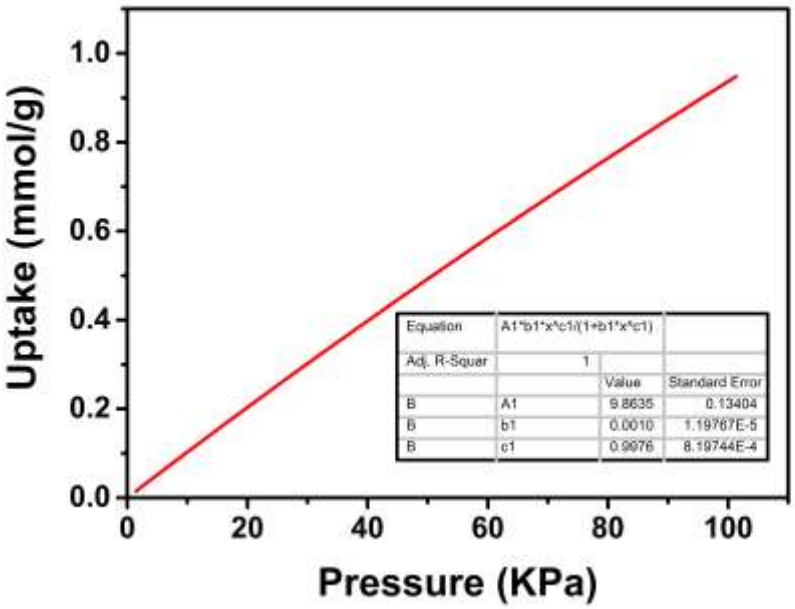


**Figure S57. UPC-102-Zr**: the parameters and optimized adsorption isotherms of $CH_4$ for calculated selectivity by using Ideal Adsorbed Solution Theory (IAST) at 273 K.

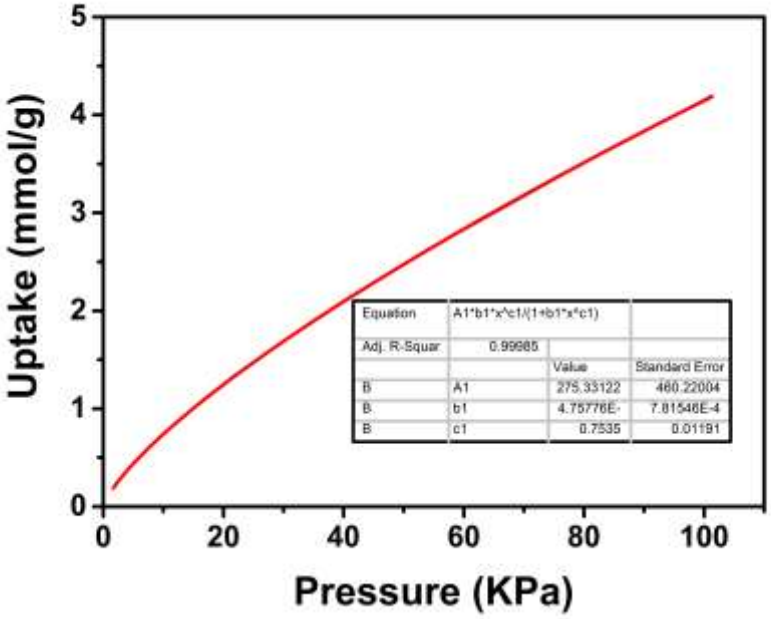


**Figure S58. UPC-102-Zr**: the parameters and optimized adsorption isotherms of $C_2H_2$ for calculated selectivity by using Ideal Adsorbed Solution Theory (IAST) at 273 K.

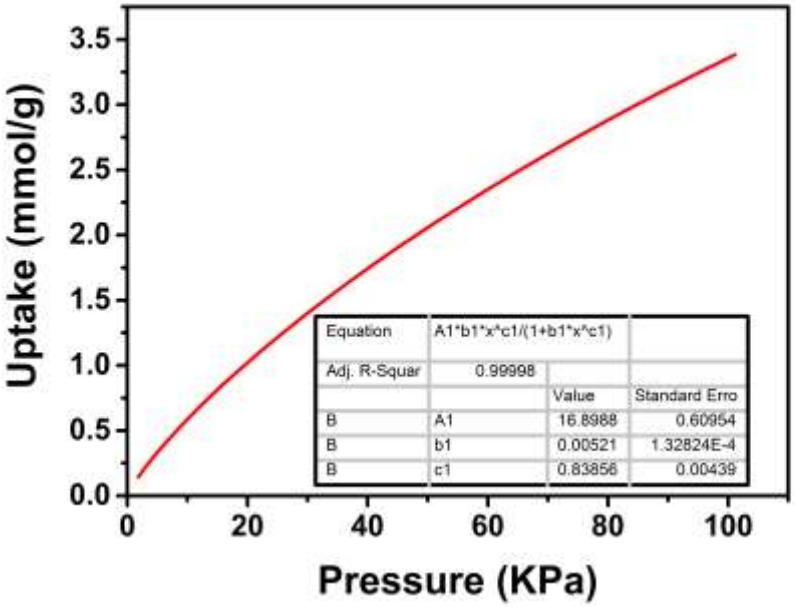


**Figure S59. UPC-102-Zr**: the parameters and optimized adsorption isotherms of $C_2H_4$ for calculated selectivity by using Ideal Adsorbed Solution Theory (IAST) at 273 K.

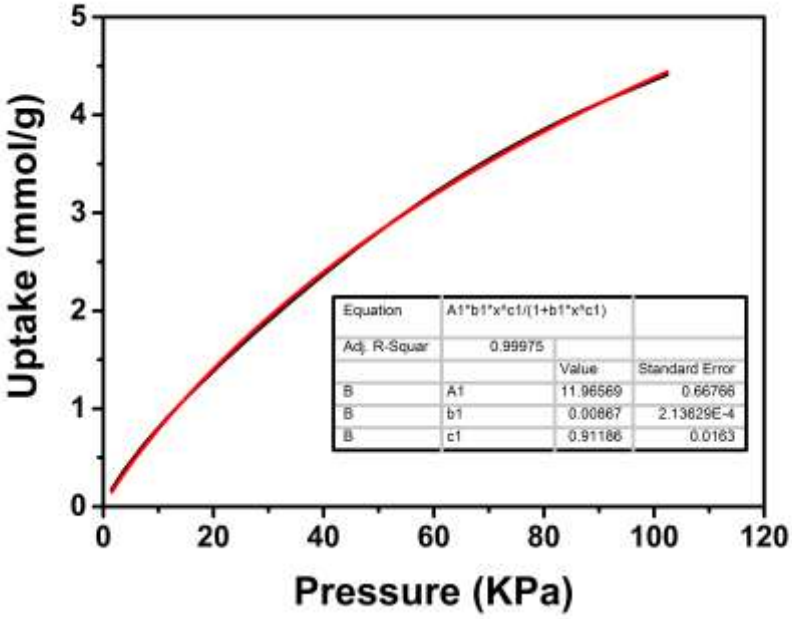


**Figure S60. UPC-102-Zr**: the parameters and optimized adsorption isotherms of $C_2H_6$ for calculated selectivity by using Ideal Adsorbed Solution Theory (IAST) at 273 K.

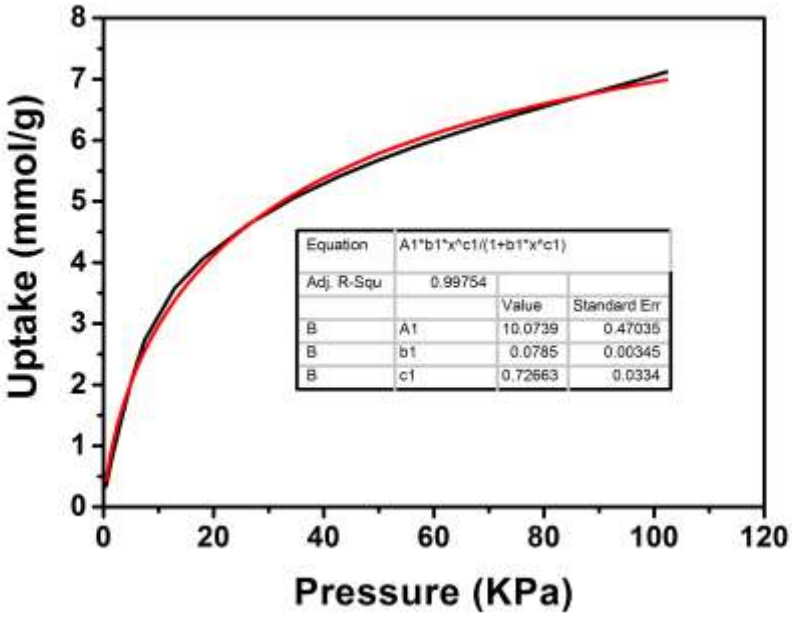


**Figure S61. UPC-102-Zr**: the parameters and optimized adsorption isotherms of $C_3H_6$ for calculated selectivity by using Ideal Adsorbed Solution Theory (IAST) at 273 K.

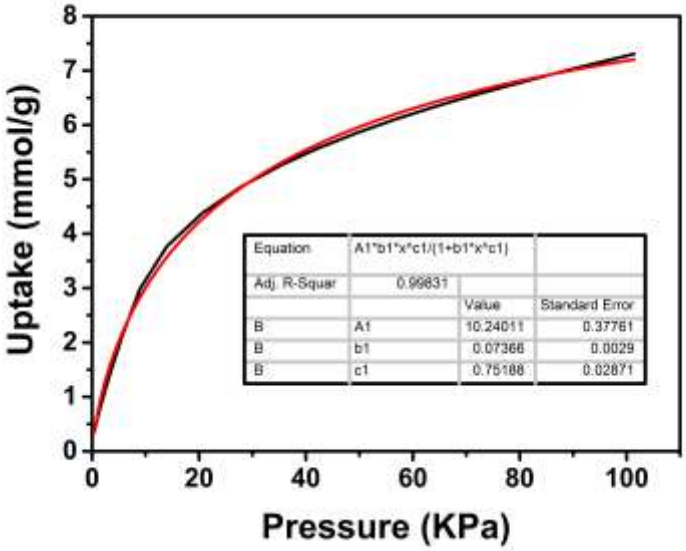


**Figure S62. UPC-102-Zr**: the parameters and optimized adsorption isotherms of $C_3H_8$ for calculated selectivity by using Ideal Adsorbed Solution Theory (IAST) at 273 K.

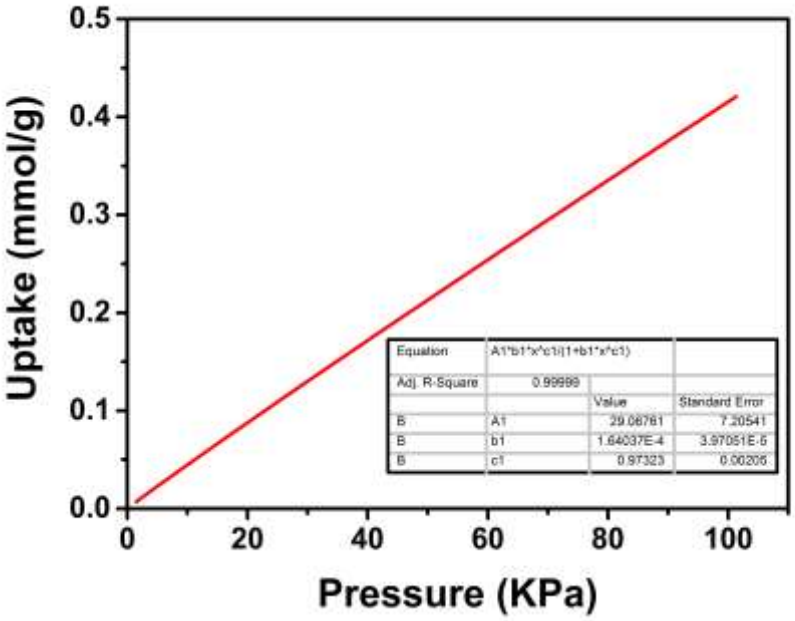


**Figure S63. UPC-102-Zr**: the parameters and optimized adsorption isotherms of $CH_4$ for calculated selectivity by using Ideal Adsorbed Solution Theory (IAST) at 298 K.

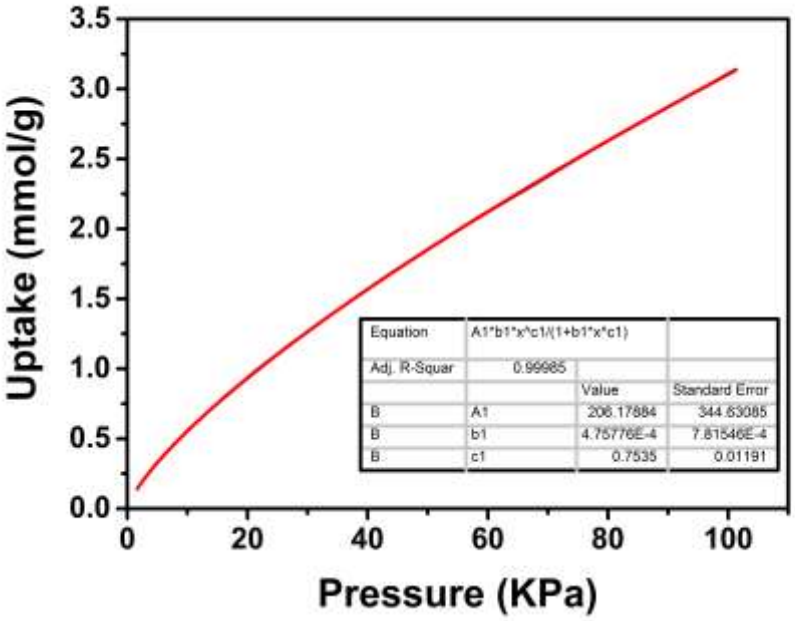


**Figure S64. UPC-102-Zr**: the parameters and optimized adsorption isotherms of $C_2H_2$ for calculated selectivity by using Ideal Adsorbed Solution Theory (IAST) at 298 K.

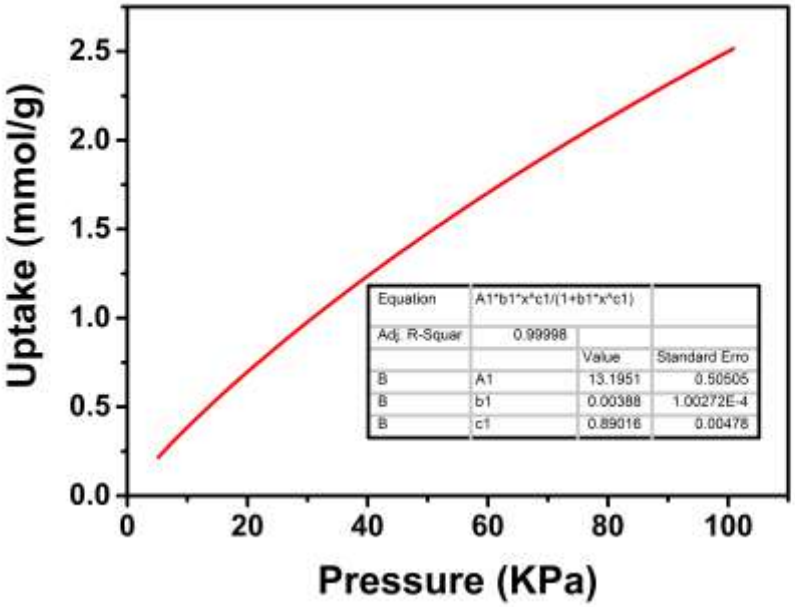


**Figure S65. UPC-102-Zr**: the parameters and optimized adsorption isotherms of $C_2H_4$ for calculated selectivity by using Ideal Adsorbed Solution Theory (IAST) at 298 K.

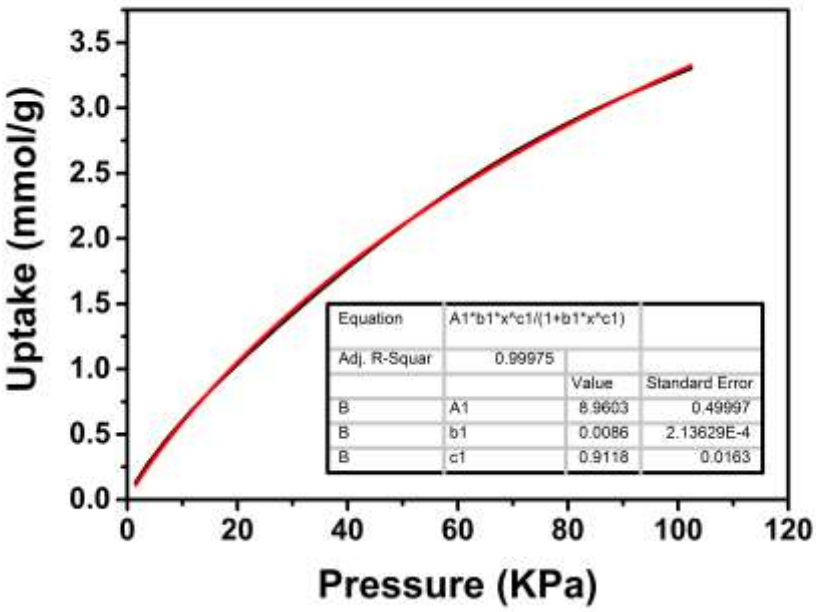


**Figure S66. UPC-102-Zr**: the parameters and optimized adsorption isotherms of $C_2H_6$ for calculated selectivity by using Ideal Adsorbed Solution Theory (IAST) at 298 K.

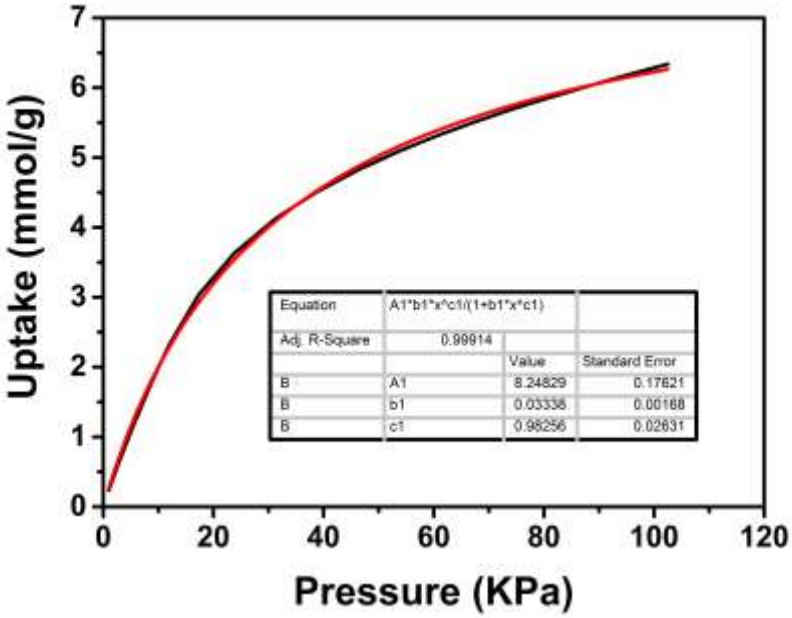


**Figure S67. UPC-102-Zr**: the parameters and optimized adsorption isotherms of $C_3H_6$ for calculated selectivity by using Ideal Adsorbed Solution Theory (IAST) at 298 K.

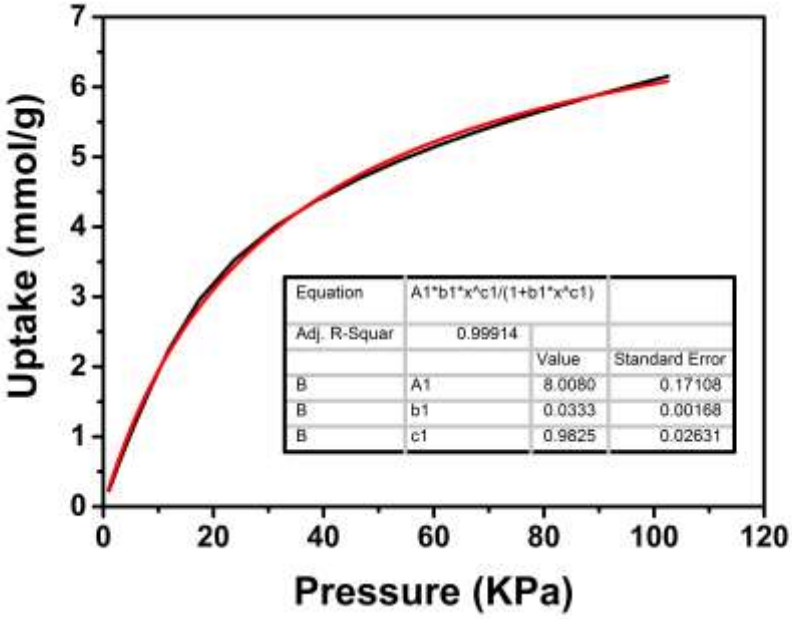


**Figure S68. UPC-102-Zr**: the parameters and optimized adsorption isotherms of $C_3H_8$ for calculated selectivity by using Ideal Adsorbed Solution Theory (IAST) at 298 K.

## 4. Dye adsorption of UPC-102-Zr.

**Table S12. Molecular weight and dimensions of guest dye molecules with different charges.**

| | | | | | |
|---|---|---|---|---|---|
| Structure | 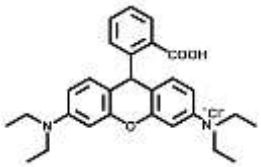 | 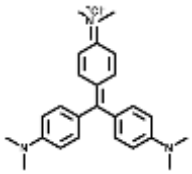 | 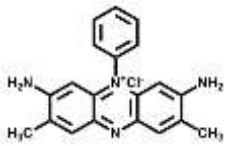 | 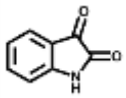 | 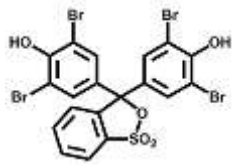 |
| 3D structure | 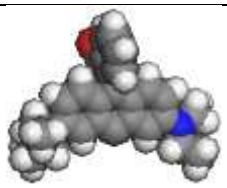 | 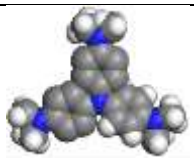 | 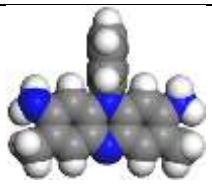 |  |  |
| name | Rhodamine B | Crystal violet | Saffron red | Isatin | Bromophenol Blue |
| Abbr.* | RHB | CV | SFR | IT | BPB |
| Z | +1 | +1 | +1 | 0 | 0 |
| $M_W$ | 480.02 | 407.98 | 350.84 | 147.13 | 669.96 |
| γ(nm) | 552 | 579 | 530 | 609 | 589 |
| x(Å) | 6.53 | 4.77 | 4.42 | 0.9 | 10.81 |
| y(Å) | 11.89 | 12.43 | 11.12 | 6.9 | 10.05 |
| z(Å) | 15.55 | 13.09 | 13.15 | 5.10 | 7.62 |
| Structure | 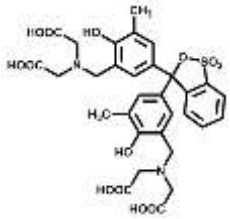 | 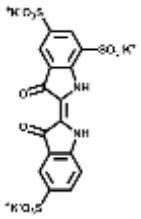 | 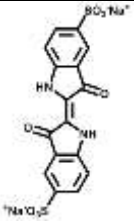 | 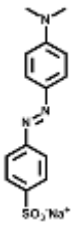 | 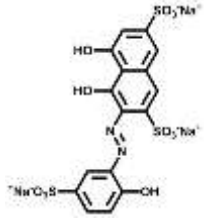 |
| 3D structure | 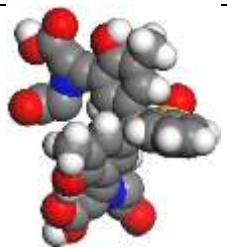 | 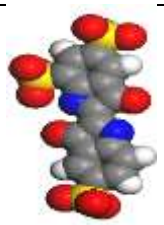 | 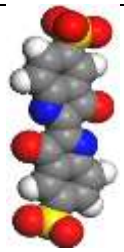 |  | 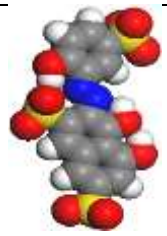 |
| name | Xylenol orange | Potassium | Indigo Carmine | Methyl | K Chrome Blue K |
| Abbr.* | XO | PTS | IC | MO | CBK |
| Z | 0 | -3 | -2 | -1 | -3 |
| $M_W$ | 672.66 | 616.72 | 466.35 | 327.33 | 586.41 |
| γ(nm) | 580 | 601 | 608 | 463 | 541 |
| x(Å) | 8.86 | 4.26 | 4.25 | 4.14 | 4.48 |
| y(Å) | 10.02 | 6.23 | 5.25 | 5.65 | 8.6 |
| z(Å) | 14.17 | 15.26 | 15.18 | 13.65 | 14.82 |

**A typical procedure for the adsorption experiments of dyes**

Taking Rhodamine B as an example, **UPC-102-Zr** (20 mg) was added into a 4 mL aqueous solution of Rhodamine B (26.3 mg $L^{-1}$) at room temperature for 12 h. The solution was centrifugated and the solution was diluted to the appropriate concentrations and analyzed by UV-Vis absorption spectroscopy. The amount of adsorbed RHB was calculated from the following mass balance equation:

$$Q_{ad} = \frac{(C_0 - C_{ad})\mathrm{V}}{\mathrm{m}}$$

where $Q_{ad}$(mg $g^{-1}$) is the amount of adsorbed RHB by adsorbent **UPC-102-Zr**, $C_0$ is the initial concentration of RHB in the water (mg $L^{-1}$), $C_{ad}$ is the concentration of RHB after adsorption (mg $L^{-1}$), V is the volume of the solution (L), and m is the mass of adsorbent **UPC-102-Zr** (g).

**Table S13. The Brunauer–Emmett–Teller (BET) surface areas of dyes@UPC-102-Zr.**

| **dyes@UPC-102-Zr** | RHB@**UPC-102-Zr** | CV@**UPC-102-Zr** | SFR@**UPC-102-Zr** | IT@**UPC-102-Zr** | BPB@**UPC-102-Zr** |
|---|---|---|---|---|---|
| $S_{BET}$ [$m^2$ $g^{-1}$] | 4.3 | 15.6 | 22.1 | 56.1 | 16.9 |
| **dyes@UPC-102-Zr** | XO@**UPC-102-Zr** | PTS@**UPC-102-Zr** | IC@**UPC-102-Zr** | MO@**UPC-102-Zr** | CBK@**UPC-102-Zr** |
| $S_{BET}$ [$m^2$ $g^{-1}$] | 131.0 | 45.2 | 19.0 | 8.6 | 34.3 |

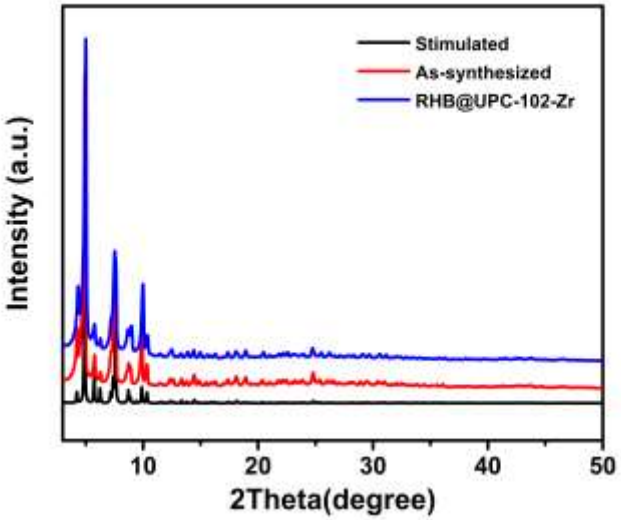


**Figure S69.** The powder X-ray diffraction (PXRD) of **RHB@UPC-102-Zr**.

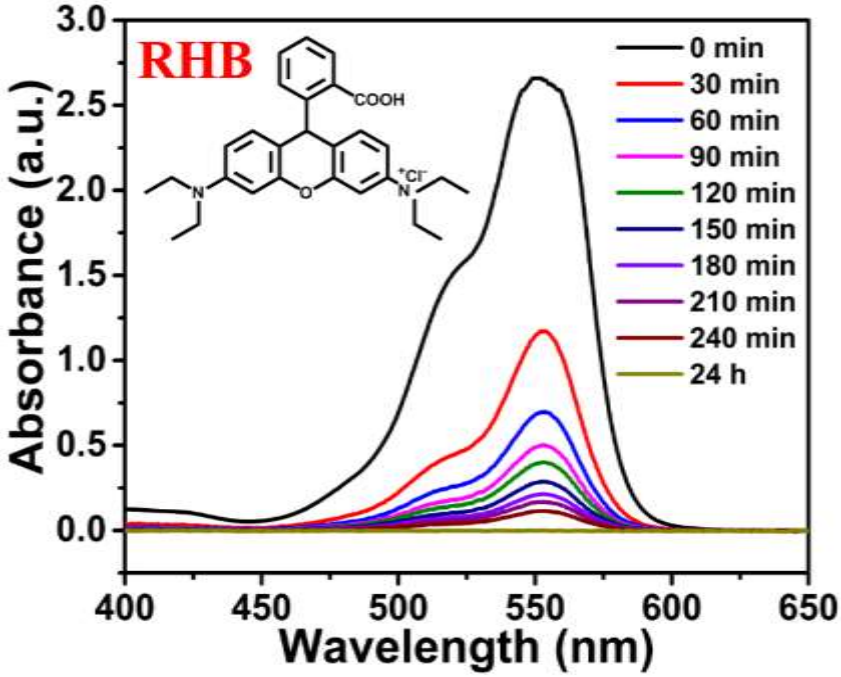


**Figure S70.** UV-vis spectra changes of RHB solution with the presence of UPC-102-Zr.

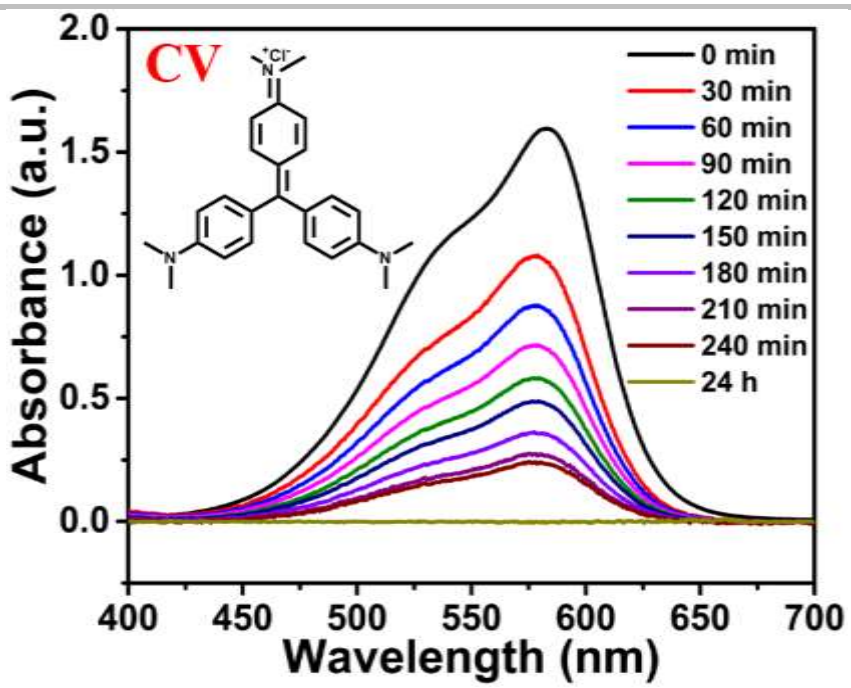


**Figure S71.** UV-vis spectra changes of CV solution with the presence of UPC-102-Zr.

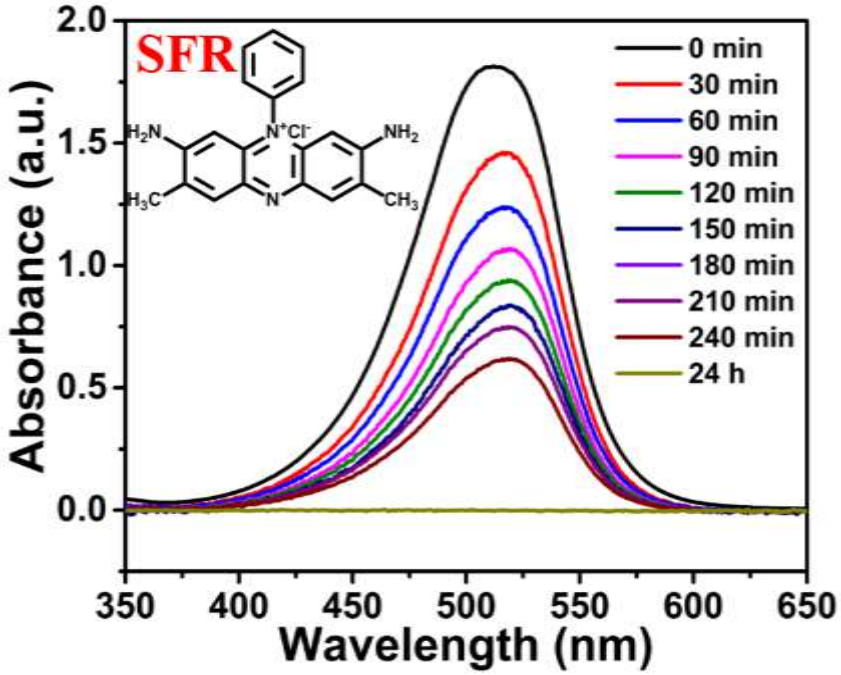


**Figure S72.** UV-vis spectra changes of SFR solution with the presence of UPC-102-Zr.

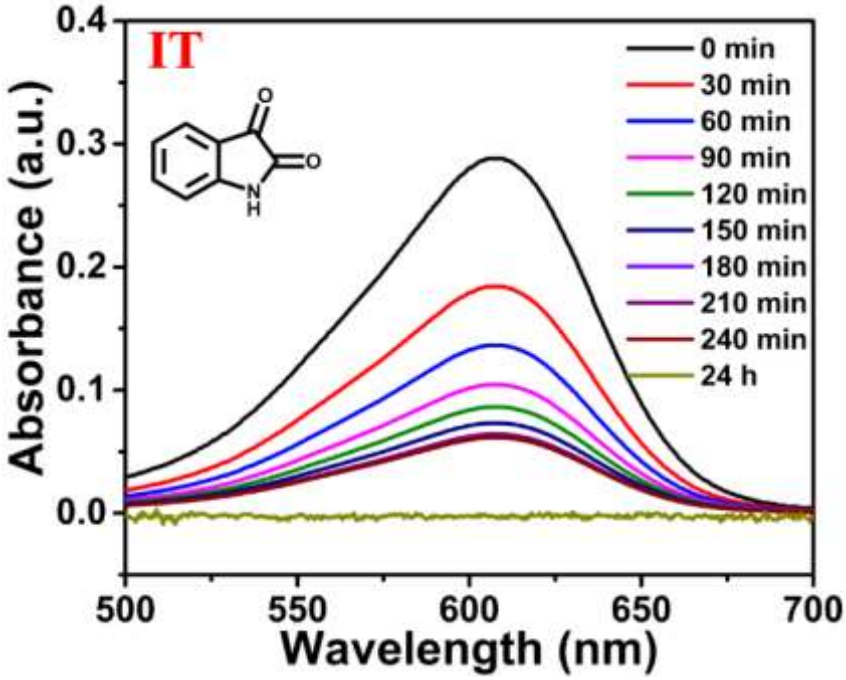


**Figure S73.** UV-vis spectra changes of IT solution with the presence of **UPC-102-Zr**.

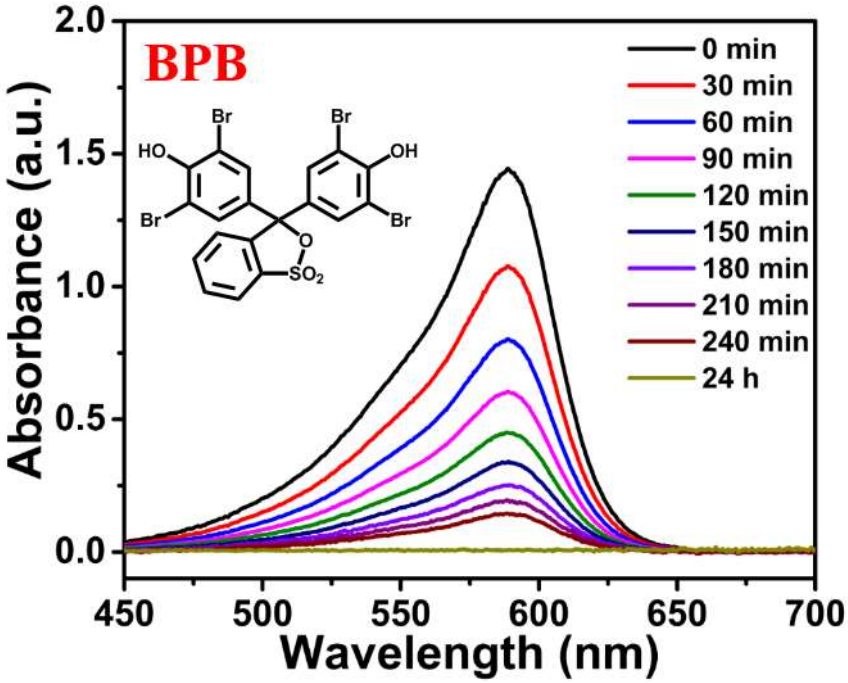


**Figure S74.** UV-vis spectra changes of BPB solution with the presence of **UPC-102-Zr**.

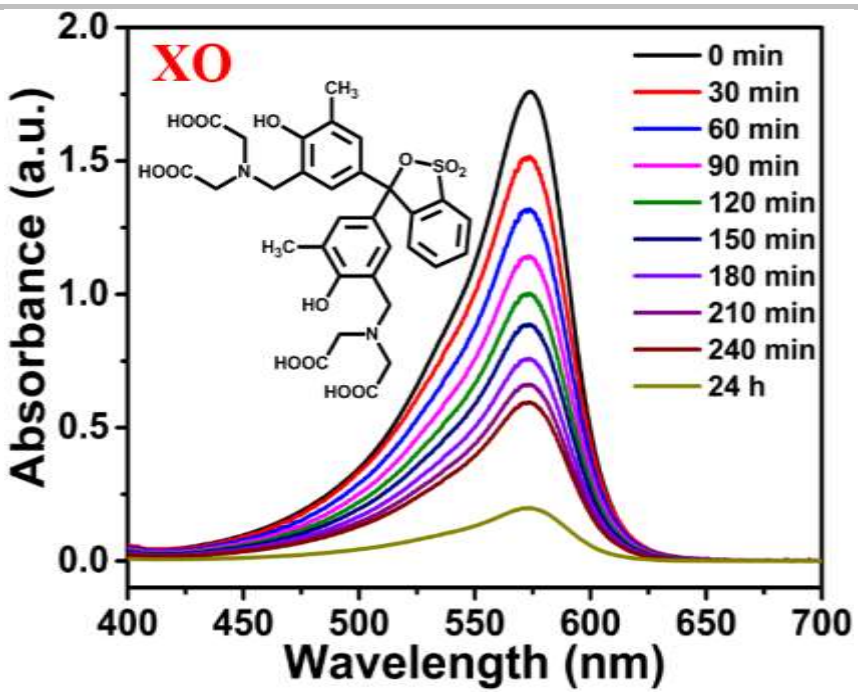


**Figure S75.** UV-vis spectra changes of XO solution with the presence of **UPC-102-Zr**.

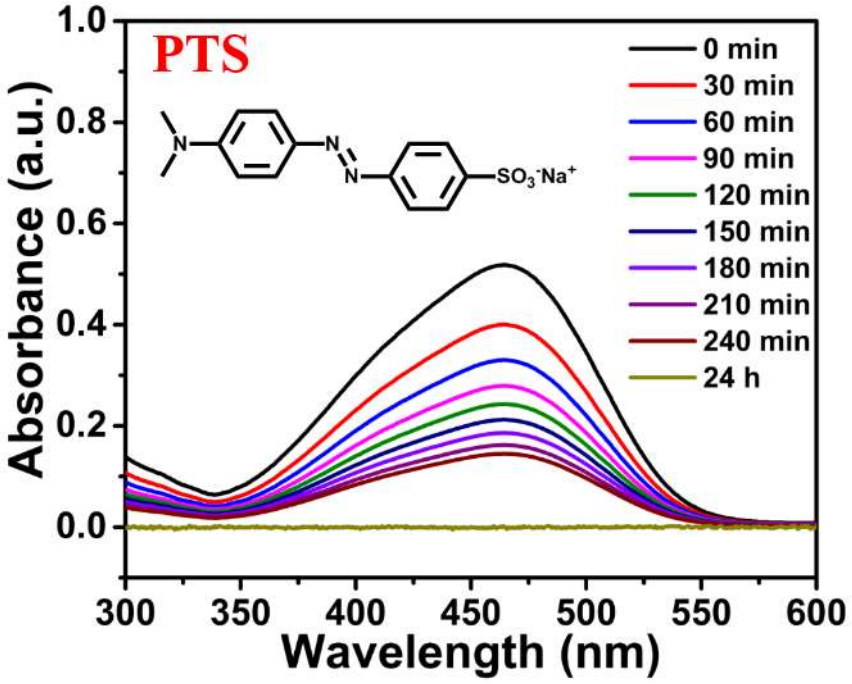


**Figure S76.** UV-vis spectra changes of PTS solution with the presence of **UPC-102-Zr**.

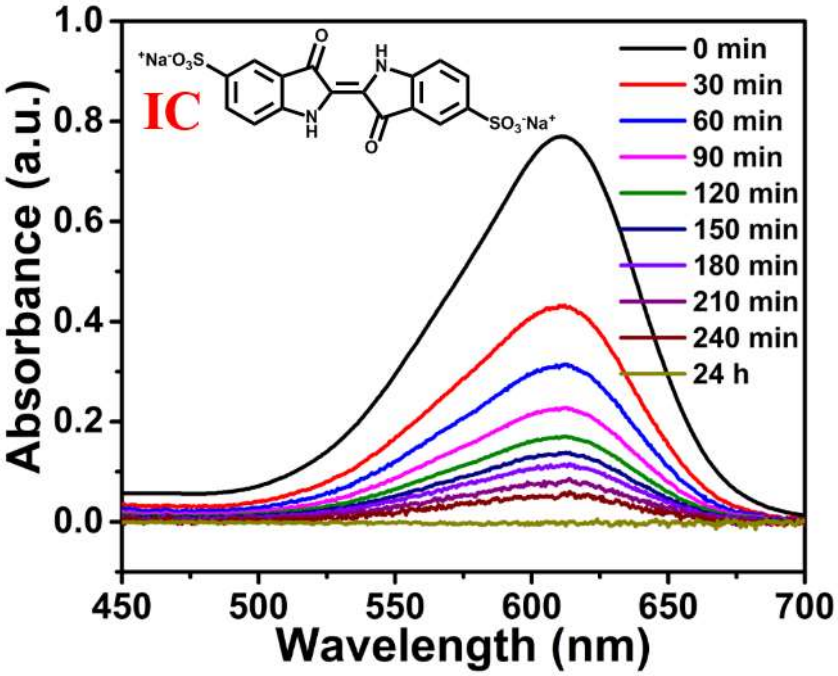


**Figure S77.** UV-vis spectra changes of IC solution with the presence of **UPC-102-Zr**.

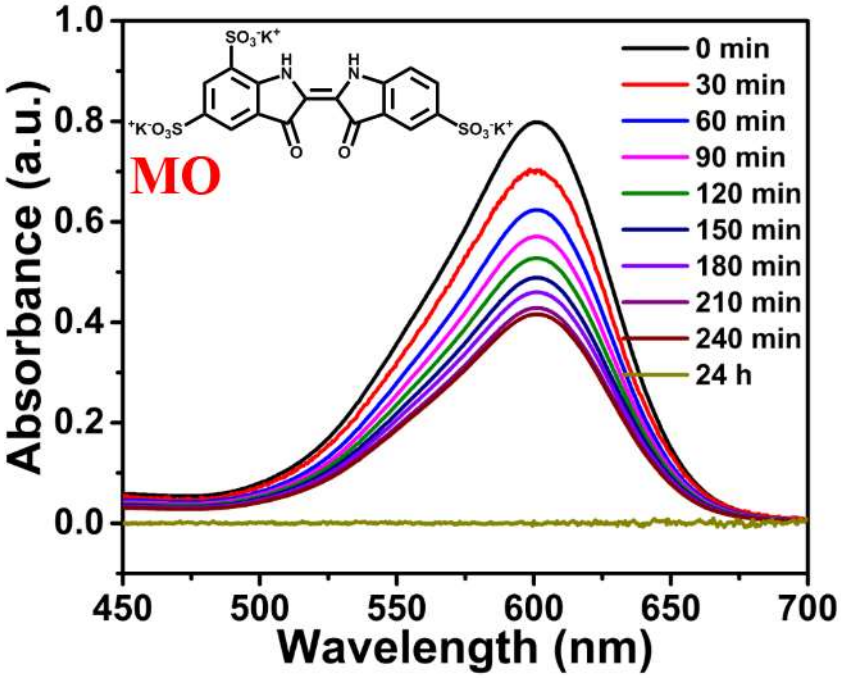


**Figure S78.** UV-vis spectra changes of MO solution with the presence of **UPC-102-Zr**.

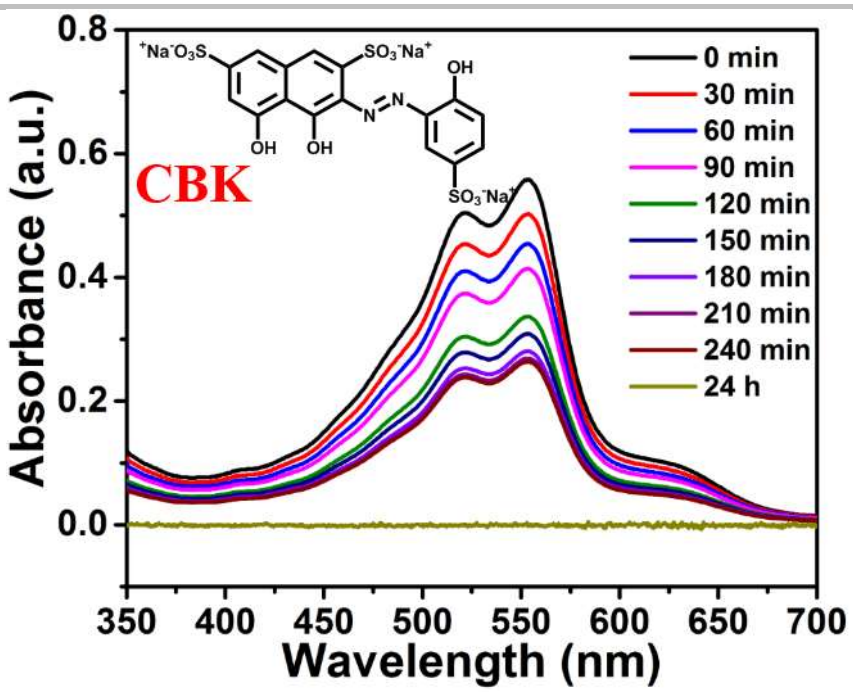


**Figure S79**. UV-vis spectra changes of CBK solution with the presence of **UPC-102-Zr**.

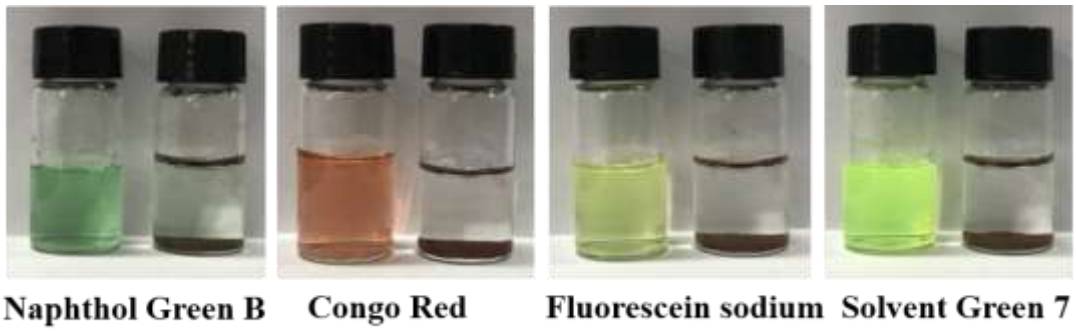


**Figure S80**. Photographs of solution before and after dye adsorption with UPC-102-Zr samples for 24 hours.

We used **UPC-102-Zr** to adsorb the large dye molecule of Naphthol Green B, Congo Red, Fluorescein sodium, and Solvent Green 7, and it can be seen from the optical photographs before and after adsorption that these large dye molecules are almost completely absorbed.

## 5. Catalyze Knoevenagel condensation reactions of UPC-100-In, UPC-101-Al, and UPC-102-Zr.

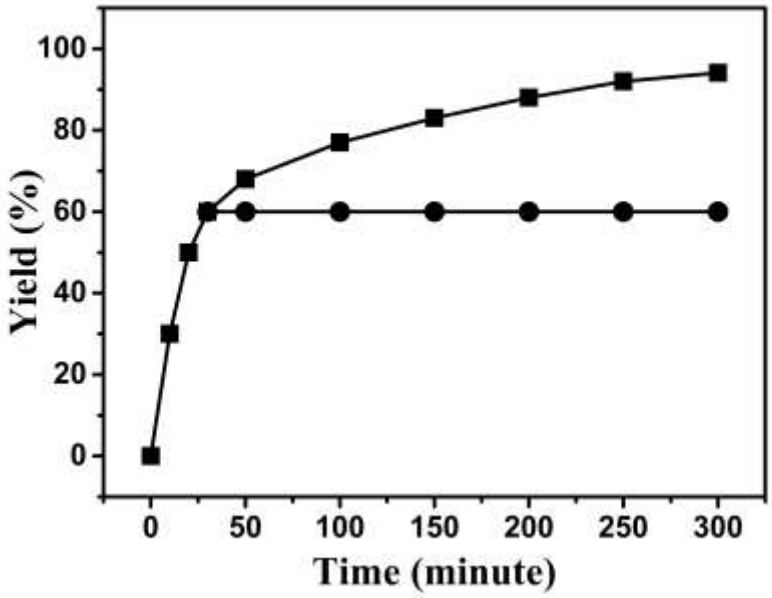


**Figure S81.** Evidence of heterogeneous nature of catalysis in Knoevenagel reaction of benzaldehyde. (■)Continuous reaction; (●)catalyst was removed after 30 minute.

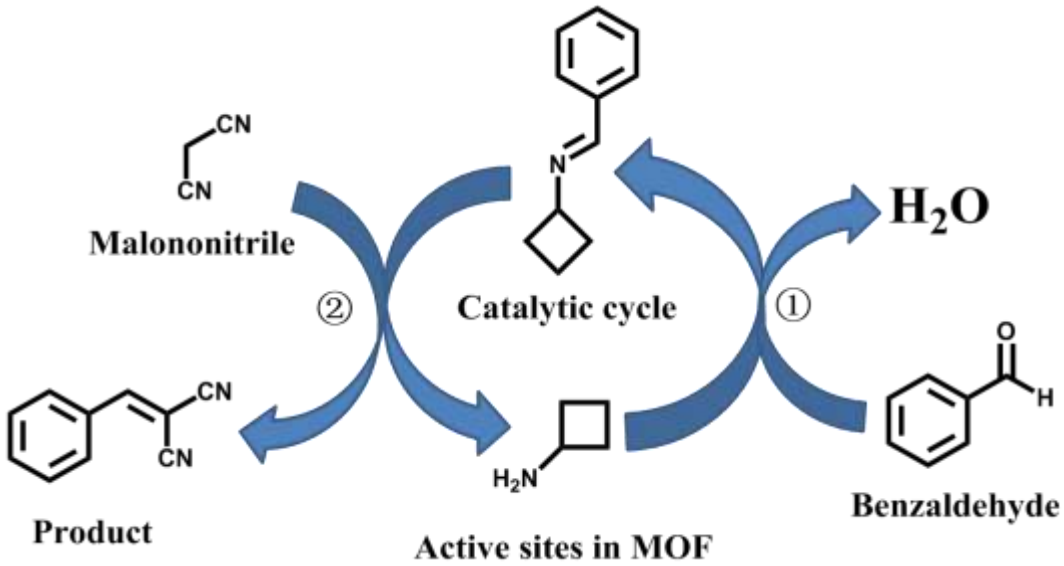


**Figure S82**. Catalytic reaction mechanism for the Knoevenagel condensation.

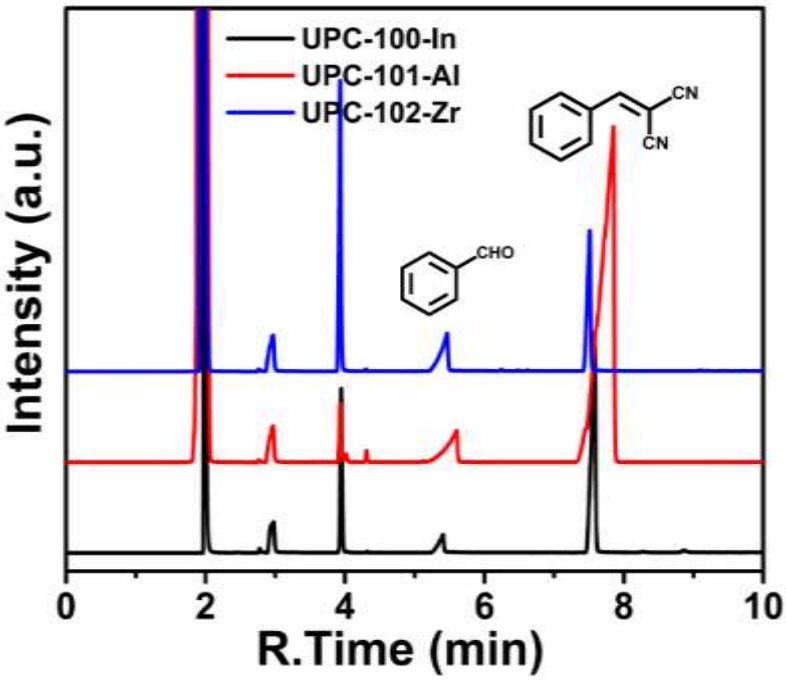


**Figure S83**. The GC spectrum for heterogeneous nature of catalysis in Knoevenagel reaction of 2-benzylidenemalononitrile. **MS** $[M+H]^+$: 153.0411.

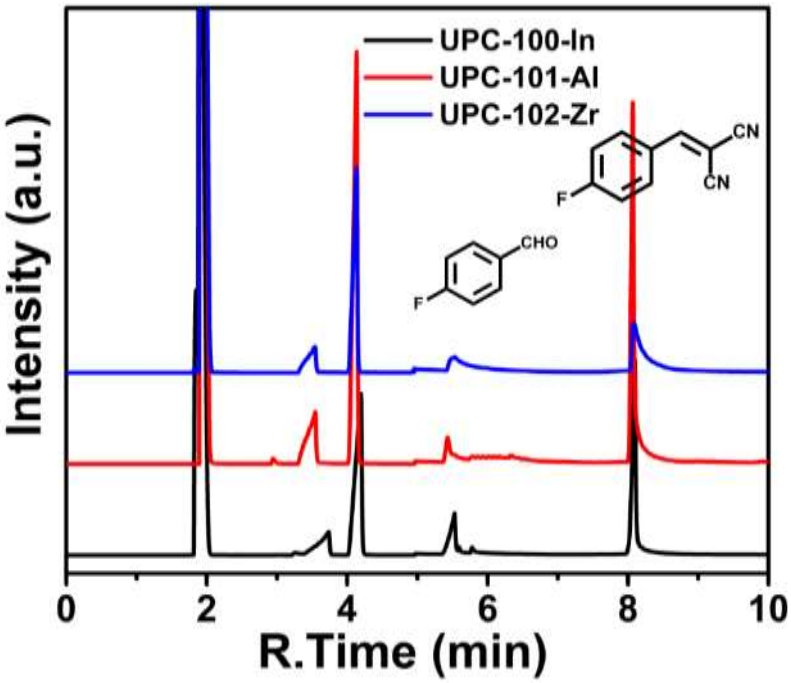


**Figure S84**. The GC spectrum for heterogeneous nature of catalysis in Knoevenagel reaction of 2-(4-fluorobenzylidene)malononitrile. **MS** $[M+H]^+$: 171.0481.

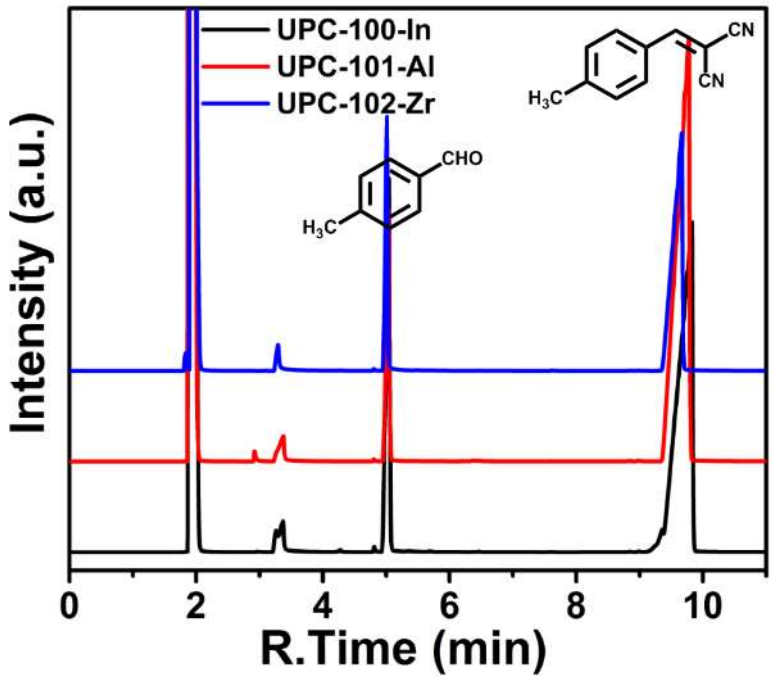


**Figure S85**. The GC spectrum for heterogeneous nature of catalysis in Knoevenagel reaction of 2-(4-methylbenzylidene)malononitrile. **MS** $[M+H]^+$: 167.0518.

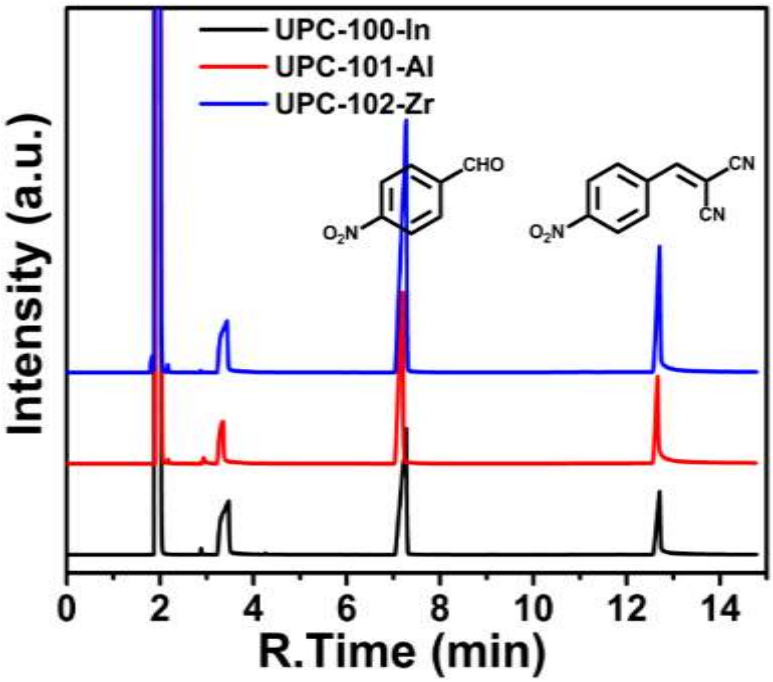


**Figure S86**. The GC spectrum for heterogeneous nature of catalysis in Knoevenagel reaction of 2-(4-nitrobenzylidene)malononitrile. **MS** $[M+H]^+$: 198.0313.

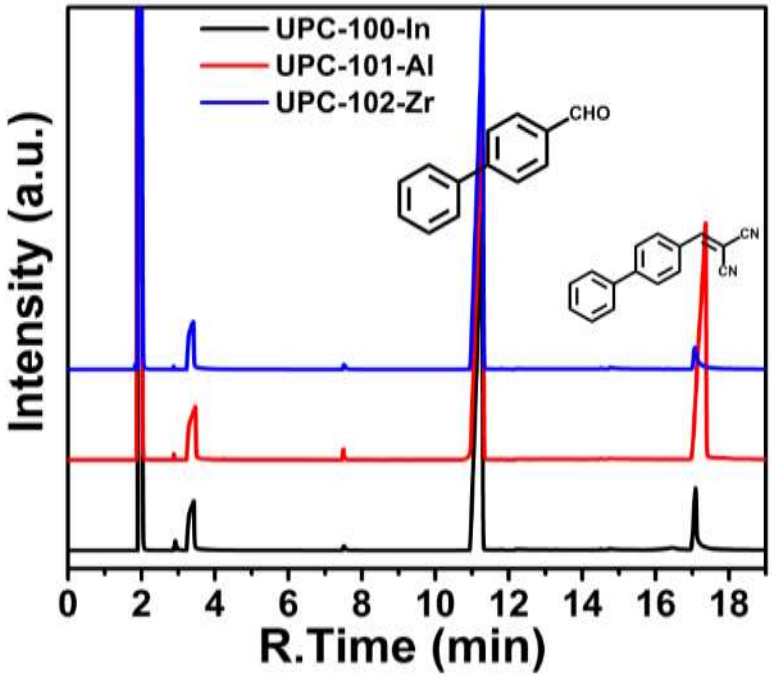


**Figure S87**. The GC spectrum for heterogeneous nature of catalysis in Knoevenagel reaction of 2-([1,1'-biphenyl]-4-ylmethylene)malononitrile. **MS** $[M+H]^+$: 181.0754.

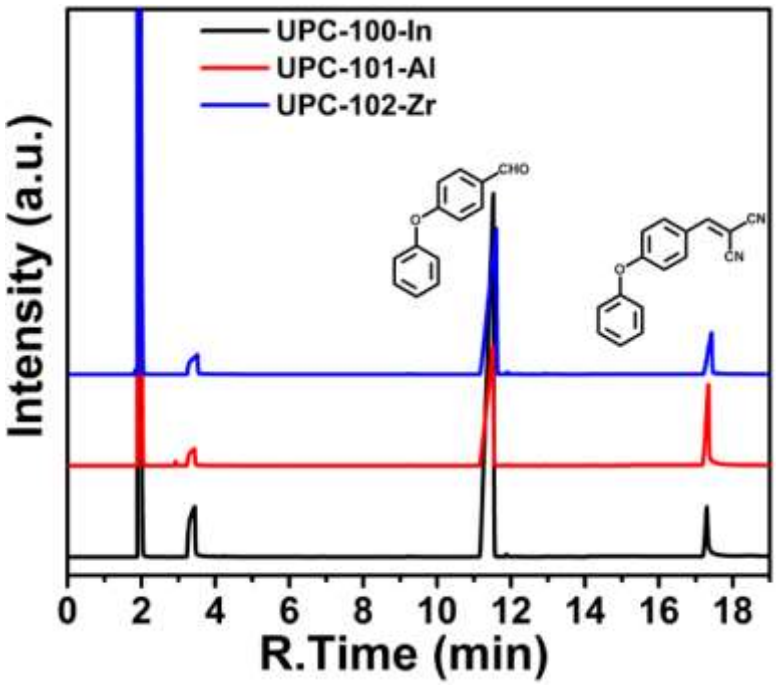


**Figure S88**. The GC spectrum for heterogeneous nature of catalysis in Knoevenagel reaction of 2-(4-phenoxybenzylidene)malononitrile. **MS** $[M+H]^+$: 245.0836.

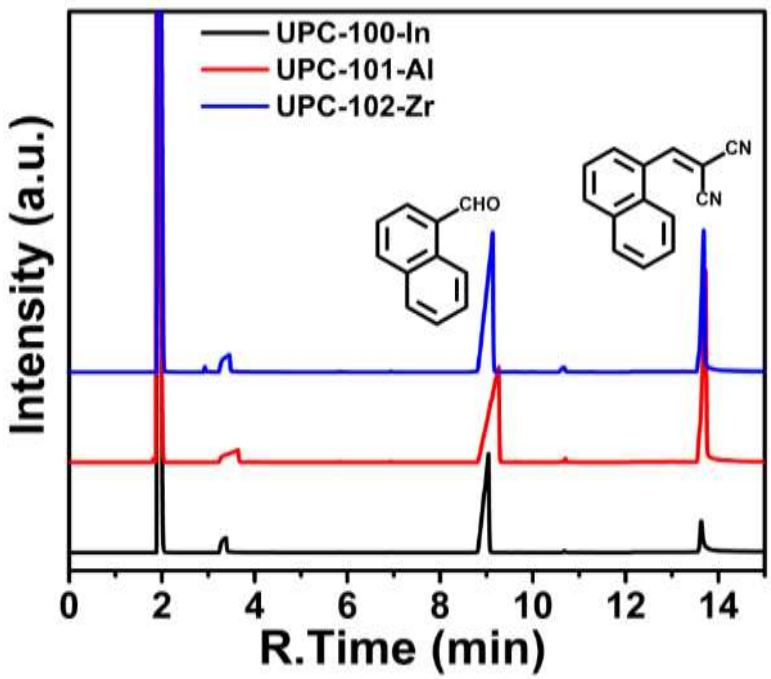


**Figure S89**. The GC spectrum for heterogeneous nature of catalysis in Knoevenagel reaction of 2-(naphthalen-1-ylmethylene)malononitrile. **MS** $[M+H]^+$: 203.0689.

## References

1. I. A. Ibarra, S. Yang, X. Lin, A. J. Blake, P. J. Rizkallah, H. Nowell, D. R. Allan, N. R. Champness and P. Hubberstey, *Chem. Commun*., 2011, **47**, 8304.

2. S. M. Humphrey, J.-S. Chang, S. H. Jhung, J. W. Yoon and P. T. Wood, *Angew. Chem. Int. Ed*., 2007, **46**, 272.

3. Y.-G. Lee, H. R. Moon, Y. E. Cheon and M. P. Suh, *Angew. Chem. Int. Ed*., 2008, **47**, 7741.

4. H. J. Park, M. P. Suh, *Chem. Eur. J*., 2008, **14**, 8812.

5. K. S. Park, Z. Ni, A. P. Cote, J. Y. Choi, R. Huang, F. J. UribeRomo, H. K. Chae, M. O'Keeffe and O. M. Yaghi, Proc. Natl. Acad. Sci. U.S.A. 2006, 103, 10186.

6. Y.-G. Lee, H. R. Moon, Y. E. Cheon and M. P. Suh, *Angew. Chem. Int. Ed*., 2008, **47**, 7741.

7. S. Barman, H. Furukawa, O. Blacque, K. Venkatesan, O. M. Yaghi and H. Berke, *Chem. Commun*., 2010, **46**, 7981.

8. J. L. C. Rowsell, A. R. Millward, K. S. Park and O. M. Yaghi, *J. Am. Chem. Soc*., 2004, **126**, 5666.

9. J. L. C. Rowsell, O. M. Yaghi, *J. Am. Chem. Soc*., 2006, **128**, 1304.

10. Y. E. Lee, S. Y. Jang and M. P. Suh, *J. Am. Chem. Soc*., 2005, **127**, 6374.

11. H. J. Park, D.-W. Lim, W. S. Yang, T.-R. Oh and M. P. Suh, *Chem. Eur. J.*, 2011, **17**, 7251.

12. D. Han, F.-L. Jiang, M.-Y. Wu, L. Chen, Q.-X. Chen and M.-C. Hong, *Chem. Commun*., 2011, **47**, 9861.

13. K. Sumida, C. M. Brown, Z. R. Herm, S. Chavan, S. Bordiga and J. R. Long, *Chem. Commun*., 2011, **47**, 1157.

14. S. Ma, H.-C. Zhou, *J. Am. Chem. Soc.*, 2006, **128**, 11734.

15. D. Sun, S. Ma, Y. Ke, D. J. Collins and H.-C. Zhou, *J. Am. Chem. Soc*., 2006, **128**, 3896.

16. H.-C. Zhou, S. Q. Ma, D. F. Sun, M. Ambrogio, J. A. Fillinger and S. Parkin, *J. Am. Chem. Soc*., 2007, **129**, 1858.

17. A. G. Wong-Foy, O. Lebel and A. J. Matzger, *J. Am. Chem. Soc*., 2007, **129**, 15740.

18. M. Kramer, U. Schwarz, S. Kaskel, *J. Mater. Chem*., 2006, **16**, 2245.

19. P. Zhang, B. Li, Y. Zhao, X. Meng and T. Zhang, *Chem. Commun*., 2011, **47**, 7722.

20. B. Chen, N. W. Ockwig, A. R. Millward, D. S. Contreras and O. M. Yaghi, *Angew. Chem. Int. Ed*., 2005, **44**, 4745.

21. X. Lin, J. Jia, X. Zhao, K. M. Thomas, A. J. Blake, G. S. Walker, N. R. Champness, P. Hubberstey and M. Schröder, *Angew. Chem. Int. Ed*., 2006, **45**, 7358.

22. X. Lin, I. Telepeni, A. J. Blake, A. Dailly, C. M. Brown, J. M. Simmons, M. Zoppi, G. S. Walker, K. M. Thomas, T. J. Mays, P. Hubberstey, N. R. Champness and M. Schröder, *J. Am. Chem. Soc*., 2009, **131**, 2159.

23. S. H. Yang, X. Lin, A. Dailly, A. J. Blake, P. Hubberstey, N. R. Champness and M. Schröder, *Chem. Eur. J*., 2009, **15**, 4829.

24. X.-S. Wang, S. Ma, P. M. Forster, D. Yuan, J. Eckert, J. L. Lopez, B. J. Murphy, J. B. Parise and H.-C. Zhou, *Angew. Chem. Int. Ed*., 2008, **47**, 7263.

25. S. Ma, J. M. Simmons, D. Sun, D. Yuan and H. Zhou, C. *Inorg. Chem*., 2009, **48**, 5263.

26. D. Sun, S. Ma, J. M. Simmons, J.-R. Li, D. Yuan and H.-C. Zhou, *Chem. Commun*., 2010, **46**, 1329.

27. W. Zhuang, S. Ma, X.-S. Wang, D. Yuan, J.-R. Li, D. Zhao and H.-C. Zhou, *Chem. Commun.*, 2010, **46**, 5223.

28. D. Zhao, D. Yuan, A. Yakovenko, H.-C. Zhou, *Chem. Commun*., 2010, **46**, 4196.

29. Y.-G. Lee, H. R. Moon, Y. E. Cheon and M. P. Suh, *Angew. Chem. Int. Ed*., 2008, **47**, 7741.

30. T. K. Kim, M. P. Suh, *Chem. Commun*., 2011, **47**, 4258.

31. T. K. Prasad, D. H. Hong, M. P. Suh, *Chem. Eur. J.*, 2010, **16**, 14043.

32. Z. Guo, H. Wu, G. Srinivas, Y. Zhou, S. Xiang, Z. Chen, Y. Yang, W. Zhou, M. O'Keeffe and B. Chen, *Angew. Chem. Int. Ed*., 2011, **50**, 3178.

33. D. Yuan, D. Zhao, D. Sun, H.-C. Zhou, *Angew. Chem. Int. Ed*., 2010, **49**, 5357.

34. Y. Yan, S. Yang, A. J. Blake, W. Lewis, E. Poirier, S. A. Barnett, N. R. Champness and M. Schröder, *Chem. Commun*., 2011, **47**, 9995.

35. D. Yuan, D. Zhao, H.-C. Zhou, *Inorg. Chem*., 2011, **50**, 10528–10530.

36. O. K. Farha, A. O. Yazaydin, I. Eryazici, C. D. Malliakas, B. G. Hauser, M. G. Kanatzidis, S. T. Nguyen, R. Q. Snurr and J. T. Hupp, *Nat. Chem*., 2010, **2**, 944.

37. S. Hong, M. Oh, M. Park, J. W. Yoon, J. S. Chang and M. S. Lah, *Chem. Commun*., 2009, **45**, 5397.

38. C. Tan, S. Yang, N. R. Champness, X. Lin, A. J. Blake, W. Lewis and M. Schröder, *Chem. Commun*., 2011, **47**, 4487.

39. W. D. Fan, Y. T. Wang, Q. Zhang, A. Kirchon, Z. Y. Xiao, L. L. Zhang, F. N. Dai, R. M. Wang and D. F. Sun, Chem. Eur. J. 2018, 24, 2137–2143.

40. Y. B. Huang, Z.J. Lin, H. R. Fu, F. Wang, M. Shen, X. S. Wang and R. Cao. *ChemSusChem* 2014, **7**, 2647-2653.

41. L. Li, X. S. Wang, J. Liang, Y. B. Huang, H. F. Li, Z. J. Lin and R. Cao. *ACS Appl. Mater. Interfaces* 2016, **8**, 9777-9781.

42. Y. B. He, Z. J. Zhang, S. C. Xiang, F. R. Fronczek, R. Krishna, and B. L. Chen. *Chem. Eur. J.* 2012, **18**, 613-619.

43. H. R. Fu and J. Zhang. *Inorg. Chem.* 2016, **55**, 3928-3932.

44. M. H. Zhang, X. L. Xin, Z. Y. Xiao, R. M. Wang, L. L. Zhang and D. F. Sun. *J. Mater. Chem. A*, 2017, **5**, 1168-1175.

45. A. M. Plonka, X. Y. Chen, H. Wang, R. Krishna, X. L. Dong, D. Banerjee, W. R. Woerner, Y. Han, J. Li and J. B. Parise .*Chem. Mater.* 2016, **28**, 1636-1646.

46. Y. Wang, M. H. He, X. X. Gao, S. D. Li and Y. B. He. *Dalton Trans.*, 2018, **47**, 7213-7221.

47. Y. Wang, M. H. He, X. X.Gao, P. Long, Y. Y. Zhang, H. Y. Zhong, X. Wang and Y. B. He. *Dalton Trans.*, 2018, **47**, 12702-12710.

48. Y. Han, H. Zheng, K. Liu, H. L. Wang, H. L. Huang, L. H.Xie, L. Wang, and J. R. Li. *ACS Appl. Mater. Interfaces* 2016, **8**, 23331-23337.

49. Y. B. He, C. L. Song, Y. J. Ling, C. D. Wu, R. Krishna, and B. L. Chen. *APL Mater.* 2014, **2**, 124102.

50. N. Sikdar, S. Bonakala, R. Haldar, S. Balasubramanian, and T. K. Maji. *Chem. Eur. J.* 2016, **22**, 6059-6070.